

Two specific publications related to neurodegeneration disease

1. Haridevamuthu, B., Sudhakaran, G., Pachaiappan, R., Kathiravan, M.K., Manikandan, K., Almutairi, M.H., Almutairi, B.O., Arokiyaraj, S. and **Arockiaraj J***, 2024. Daidzein ameliorates nonmotor symptoms of manganese-induced Parkinsonism in zebrafish model: Behavioural and biochemical approach. *British Journal of Pharmacology*. <https://doi.org/10.1111/bph.16382> (IF – 6.8)
2. Murugan, R., Nayak, S.R.R., Haridevamuthu, B., Priya, D., Chitra, V., Almutairi, B.O., Arokiyaraj, S., Saravanan, M., Kathiravan, M.K. and **Arockiaraj J***, 2024. Neuroprotective potential of pyrazole benzenesulfonamide derivative T1 in targeted intervention against PTZ-induced epilepsy-like condition in in vivo zebrafish model. *International Immunopharmacology*, 131, p.111859. <https://doi.org/10.1016/j.intimp.2024.111859> (IF - 4.8)

See discussions, stats, and author profiles for this publication at: <https://www.researchgate.net/publication/380176124>

Daidzein ameliorates nonmotor symptoms of manganese-induced Parkinsonism in zebrafish model: Behavioural and biochemical approach

Article in *British Journal of Pharmacology* · April 2024

DOI: 10.1111/bph.16382

CITATIONS

0

READS

110

9 authors, including:



B. Haridevamuthu

Saveetha Medical College and Hospitals

62 PUBLICATIONS 439 CITATIONS

SEE PROFILE



Gokul Sudhakaran

SRM Institute of Science and Technology

54 PUBLICATIONS 375 CITATIONS

SEE PROFILE



Raman Pachaippan

SRM Institute of Science and Technology

99 PUBLICATIONS 1,537 CITATIONS

SEE PROFILE



Kathiravan Muthukumaradoss










SRM Institute of Science and Technology

62 PUBLICATIONS 254 CITATIONS

SEE PROFILE

RESEARCH ARTICLE

Daidzein ameliorates nonmotor symptoms of manganese-induced Parkinsonism in zebrafish model: Behavioural and biochemical approach

Balasubramanian Haridevamuthu¹  | Gokul Sudhakaran¹  |
 Raman Pachiappan²  | Muthu Kumaradoss Kathiravan³  |
 Krishnan Manikandan⁴  | Mikhliid H. Almutairi⁵  | Bader O. Almutairi⁵  |
 Selvaraj Arokiyaraj⁶  | Jesu Arockiaraj⁷ 

¹Center for Global Health Research, Saveetha Medical College and Hospital, Saveetha Institute of Medical and Technical Sciences (SIMATS), Chennai, Tamil Nadu, 600105, India

²Department of Biotechnology, School of Bioengineering, Faculty of Engineering and Technology, SRM Institute of Science and Technology, Kattankulathur, Chengalpattu District, Tamil Nadu, 603203, India

³Dr APJ Abdul Kalam Research Lab, Department of Pharmaceutical Chemistry, SRM College of Pharmacy, SRM Institute of Science and Technology, Kattankulathur, Chengalpattu District, Tamil Nadu, 603203, India

⁴Department of Pharmaceutical Analysis, SRM College of Pharmacy, SRM Institute of Science and Technology, Kattankulathur, Chengalpattu District, Tamil Nadu, 603203, India

⁵Department of Zoology, College of Science, King Saud University, P.O. Box 2455, Riyadh, 11451, Saudi Arabia

⁶Department of Food Science & Biotechnology, Sejong University, Seoul, 05006, Korea

⁷Toxicology and Pharmacology Laboratory, Department of Biotechnology, Faculty of Science and Humanities, SRM Institute of Science and Technology, Kattankulathur, Chengalpattu District, Tamil Nadu, 603203, India

Correspondence

Jesu Arockiaraj, Toxicology and Pharmacology Laboratory, Department of Biotechnology, Faculty of Science and Humanities, SRM

Abstract

Background and Purpose: Parkinson's disease (PD) is a prevalent neurodegenerative movement disorder characterized by motor dysfunction. Environmental factors, especially manganese (Mn), contribute significantly to PD. Existing therapies are focused on motor coordination, whereas nonmotor features such as neuropsychiatric symptoms are often neglected. Daidzein (DZ), a phytoestrogen, has piqued interest due to its antioxidant, anti-inflammatory, and anxiolytic properties. Therefore, we anticipate that DZ might be an effective drug to alleviate the nonmotor symptoms of Mn-induced Parkinsonism.

Experimental Approach: Naïve zebrafish were exposed to 2 mM of Mn for 21 days and intervened with DZ. Nonmotor symptoms such as anxiety, social behaviour, and olfactory function were assessed. Acetylcholinesterase (AChE) activity and antioxidant enzyme status were measured from brain tissue through biochemical assays. Dopamine levels and histology were performed to elucidate neuroprotective mechanism of DZ.

Key Results: DZ exhibited anxiolytic effects in a novel environment and also improved intra and inter fish social behaviour. DZ improved the olfactory function and response to amino acid stimuli in Mn-induced Parkinsonism. DZ reduced brain oxidative stress and AChE activity and prevented neuronal damage. DZ increased DA level in the brain, collectively contributing to neuroprotection.

Conclusion and Implications: DZ demonstrated a promising effect on alleviating nonmotor symptoms such as anxiety and olfactory dysfunction, through the mitigation of cellular damage. These findings underscore the therapeutic potential of DZ in addressing nonmotor neurotoxicity induced by heavy metals, particularly in the context of Mn-induced Parkinsonism.

Abbreviations: AChE, acetylcholinesterase; ATCI, acetylthiocholine iodide; AD, Alzheimer's disease; CAT, catalase; DA, dopamine; DMSO, dimethyl sulfoxide; Don, donepezil hydrochloride; DOPAC, 3,4-dihydroxyphenylacetic acid; DZ, daidzein; GPx, glutathione peroxidase; GSH, reduced glutathione; MDA, malondialdehyde; Mn, manganese; MS222, tricaine methanesulfonate; MTD, maximum tolerated dose; PD, Parkinson's disease; SOD, superoxide dismutase; TAA, time spent in the amino acid region; TNAA, time spent in the non-amino acid region.***

Institute of Science and Technology,
Kattankulathur 603203, Chengalpattu District,
Tamil Nadu, India.
Email: jesuaroa@srmist.edu.in

Funding information

Researchers Supporting Project, King Saud
University, Riyadh, Saudi Arabia, Grant/Award
Number: RSP2024R414

KEYWORDS

anxiolytic effect, daidzein, nonmotor symptoms, Parkinsonism, phytoestrogen

1 | INTRODUCTION

Parkinson's disease (PD) stands as the most prevalent neurodegenerative movement disorder, primarily distinguished by a deterioration in the coordination of movement. Beyond its motor aspects, PD is marked by nonmotor features including autonomic dysfunction and neuropsychiatric symptoms (Pyatha et al., 2022). Ranking as the second most common neurodegenerative disorder globally, following Alzheimer's disease (AD), PD is projected to experience a substantial increase in prevalence. Forecasts suggest that the worldwide prevalence of PD is expected to double by the year 2040 (Dorsey et al., 2018). This trajectory positions PD as the fastest-growing neurodegenerative disease, surpassing the anticipated rise in incidence observed for AD (Feigin et al., 2017). Epidemiological studies showed that more than 90% of PD cases are attributed to environmental factors, where heavy metals such as manganese are predominant and have been identified as a contributor to PD progression (Goldman, 2014; Pyatha et al., 2022). The common mechanisms driving Mn-induced Parkinsonism involve an imbalance in basal ganglia neurotransmitters, especially **dopamine**, leading to subsequent deficits in neurobehavioural and motor outputs. This imbalance may be associated with the initiation of oxidative stress, inflammation, and apoptotic pathways within brain regions (Abu-Elfotuh et al., 2022; Yao et al., 2021). Consequently, halting the hallmark features of PD progression, particularly oxidative stress, has the potential to interrupt a detrimental cycle, initiated by the generation of free radicals and perturbation of oxidative status, that ultimately culminates in the apoptosis of basal ganglia neurons. Addressing these key pathways may offer a potential strategy to intervene in the progression of PD-associated neurotoxicity (Abu-Elfotuh et al., 2022).

Considerable emphasis has been placed on the exploration of novel therapeutic strategies for neurodegenerative diseases, including PD. This research has primarily centred on the utilization of phytochemicals derived from plants. These compounds are of interest due to their inherent antioxidant and anti-inflammatory properties, coupled with a lower incidence of toxic effects. In that context, **daidzein** (DZ, Figure 1a), a natural plant isoflavone (IUPAC Name: 7-hydroxy-3-(4-hydroxyphenyl)chromen-4-one) is the most commonly consumed type of phytoestrogen, prevalent in nuts, fruits, soybeans, and soybean products. As a member of the 7-hydroxyisoflavone class, DZ is known for its antioxidant and anti-inflammatory properties (X. Wang et al., 2022). DZ inhibits the activation of nuclear factor kappa B (NF- κ B) and reduces inflammation in **LPS**-stimulated macrophages (Aziz et al., 2020). It has been reported that DZ exerts anxiolytic

What is already known

- Manganese (Mn) induces Parkinsonism by the activation of oxidative stress, inflammation, and apoptotic pathways.
- Daidzein (DZ) possess antioxidant, anti-inflammatory, and anxiolytic properties.

What does this study add

- DZ reduced brain oxidative stress and AChE activity, and prevented neuronal damage in Mn-induced Parkinsonism.
- DZ alleviated nonmotor symptoms such as anxiety and olfactory dysfunction in Mn-induced Parkinsonism.

What is the clinical significance

- This study highlights the therapeutic potential of DZ in addressing Mn-induced nonmotor neurotoxicity.

effects and improves motor coordination and social behaviour (Wu et al., 2022; Zeng et al., 2010). Moreover, DZ regulates redox homeostasis, restores dopamine levels, and improves the PD condition in **reserpine**-induced rats (Goel & Chaudhary, 2020). It is found to regulate the **GSK3 β** / **Nrf2** pathway and reduce neuron apoptosis in MPTP-induced mice models of PD. The role of DZ in ameliorating brain injury caused by chemically induced models like MPTP (1-methyl-4-phenyl-1,2,3,6-tetrahydropyridine), reserpine, and rotenone have been studied recently, but its protective role in Mn-induced Parkinsonism has not yet been unveiled. Based on DZ's pharmacological activities, we hypothesize that DZ could ameliorate Mn-induced Parkinsonism by reducing brain oxidative stress. Zebrafish is one of the more versatile animal models for assessing the potential therapeutic efficacy of pharmacological interventions for PD, because zebrafish brain have similar neuroanatomical and neurochemical pathways to humans (Doyle & Croll, 2022). Therefore, this study aimed to evaluate the role of DZ in alleviating the nonmotor symptoms, such as depression, anxiety, and olfactory dysfunction along with biochemical and histological alterations.

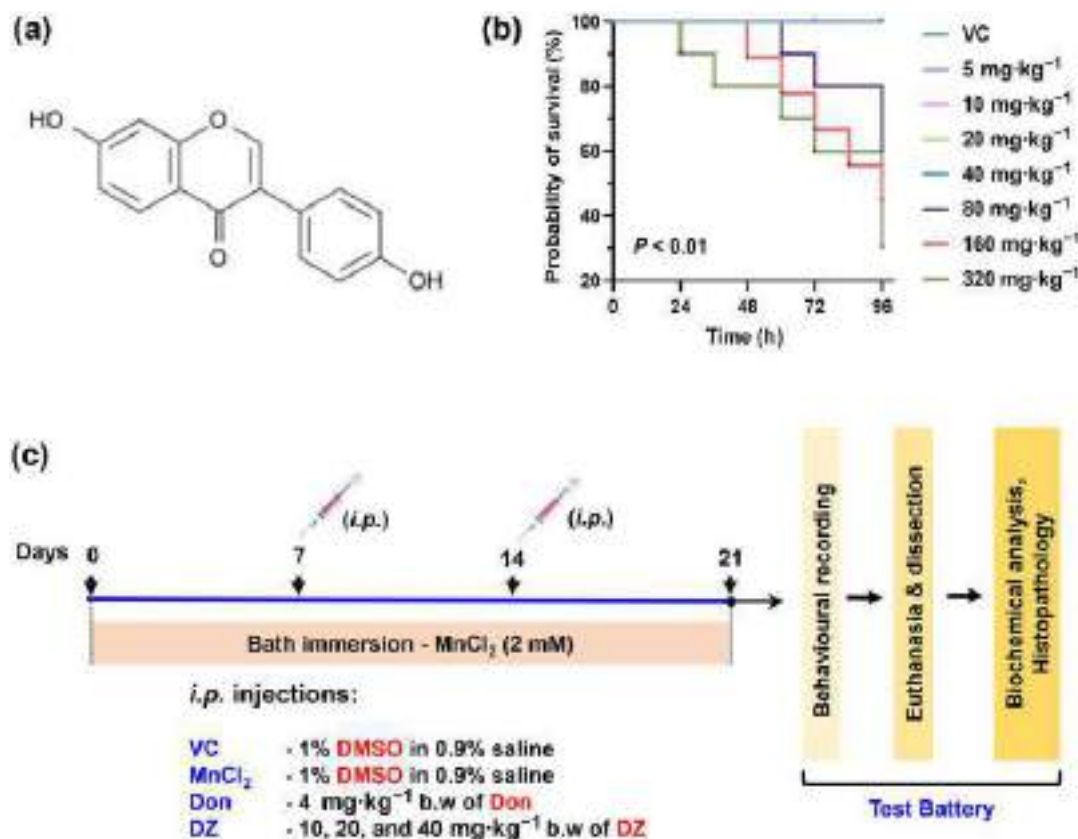


FIGURE 1 (a) Chemical structure of daidzein (DZ), (b) Kaplan-Meier survival graph of DZ (n = 10). The $P < 0.01$ represents the survival curve comparison analysed by log-rank (Mantel-Cox) test. Maximum tolerated dose (MTD) was found to be 40 mg·kg⁻¹ and used for further study. (c) Experimental paradigm of the study.

2 | METHODS

2.1 | Materials

Daidzein (DZ) (CAS# 486-66-8, purity $\geq 98\%$, 254.24 g·mol⁻¹) and Manganese (II) chloride (MnCl₂) (CAS# 7773-01-5, purity $\geq 99\%$, 125.84 g·mol⁻¹) were procured from Sigma-Aldrich (MO, USA). Donepezil hydrochloride (Don, marketed as Donecept®) is a commercial acetylcholinesterase inhibitor, purchased from Cipla Ltd., (Haridwar, India) and used as positive control (standard drug) in this study. The chemicals used in this study were purchased from Sigma-Aldrich (MO, USA) or HiMedia Laboratories (Mumbai, India) of analytical grade unless stated. Natural products studies are reported in compliance with the recommendations made by the British Journal of Pharmacology (Izzo et al., 2020). A stock solution of DZ was made by dissolving 10 mg in 30% dimethyl sulfoxide (DMSO) and further diluted in a sterile 0.9% saline solution. Don solutions were prepared directly using sterile 0.9% saline solution, and 1 g of MnCl₂ was directly dissolved in 4 L of fish water. The final concentration of DMSO in the drug injection solution did not exceed 1%. DMSO (1%) was prepared in a sterile 0.9% saline solution and used as vehicle injection. Type-1 ultrapure water from Milli-Q® Direct (MilliporeSigma, USA) was used to prepare reagents and buffers in this study.

2.2 | Animal housing

Healthy adult zebrafish (WT, *Danio rerio*), encompassing both sexes and approximately 5–6 months old with an average weight of 450 ± 40 mg, were procured from Tarun fish farm (Chennai, India). Fish were acclimatized for a period of approximately 21 days under laboratory conditions as previously described (Boopathi et al., 2023). The specified optimal parameters during acclimatization included a temperature of 27 ± 1°C, a photoperiod of 14-h light to 10-h dark (light initiated at 0800 with a 20-min dimming phase), and a stocking density of two fish per litre to meet oxygen demands. Throughout the acclimatization period, the fish were nourished with commercially available food pellets (TAIYO® Grow, India). The animal experiments strictly adhered to the Guidelines of the Committee for the Purpose of Control and Supervision of Experiments on Animals (CPCSEA) for Experimentation on Fishes (2021). Furthermore, the experimental protocol received approval from the Institutional Animal Ethics Committee of SRM College of Pharmacy (IAEC/312/2023). The process of anesthetization and killing of zebrafish was carried out in strict accordance with the Guidelines for Euthanasia of Zebrafish by Animal Research Advisory Committee (ARAC) of NIH. The experimental design, statistical analyses, and subsequent data reporting in animal studies were developed in accordance with the editorial guidelines of

British Journal of Pharmacology (Curtis et al., 2018; Lilley et al., 2020) and ARRIVE 2.0 (Percie du Sert et al., 2020) to enhance the transparency and reproducibility of research.

2.3 | Drug administration

Don and DZ were administered via the intraperitoneal (*i.p.*) route using a 31G Ultra-Fine™ II Insulin Syringe (6 mm, U-100, Becton, Dickinson and Company, India) as described in our previous study (Haridevamuthu, Seenivasan, et al., 2023). In brief, each fish was anaesthetised with buffered tricaine methanesulfonate (MS222, 100 mg·L⁻¹) until loss of motor coordination and then gently placed in a wet, soft sponge fish holder. Intraperitoneal injections were carefully administered into the midline abdominal cavity, posterior to the pelvic fins, following a standard protocol (Kinkel et al., 2010). To ensure the safety of the fish, the injection protocol was minimized to 10 s. Subsequently, the fish were transferred back to the recovery tank before being reintroduced to the experimental tank. The stock solution was diluted to accommodate the body weight of the zebrafish, with a 15-μl volume of injection. This thorough procedure was implemented to optimize the well-being of the experimental subjects.

2.4 | Acute toxicity

A preliminary acute toxicity study was conducted to determine the optimal dosage of DZ for adult zebrafish, adhering to the OECD Guidelines for the Testing of Chemicals, Section 2, Test No. 203: Fish, Acute Toxicity Test (OECD, 2019). In brief, naïve adult zebrafish ($n = 10$) were anaesthetised with buffered MS222 (100 mg·L⁻¹), and DZ was administered via *i.p.* as previously described (Kinkel et al., 2010). The dosage was selected as a geometric series, ranging from 5 to 320 mg·kg⁻¹ (5, 10, 20, 40, 80, 160, 320 mg·kg⁻¹) of body weight (b.w.), with a separation factor of two. Lethal and sublethal parameters were monitored at 24-h intervals, in accordance with OECD Test No. 203 (OECD, 2019). Kaplan–Meier survival graphs were constructed for the 96-h injection period (Figure 1b). The test fish did not exhibit any clinical signs, such as visible abnormalities in swimming behaviour, immobility, or mortality. The maximum tolerated dose (MTD) was determined to be 40 mg·kg⁻¹, prompting subsequent studies to be conducted within this MTD range.

2.5 | Experimental design

Experimentally naïve zebrafish were separated into six experimental groups in a completely randomized manner, as detailed in Table 1. A total of 96 adult zebrafish of mixed sexes were used for this study, with 16 fish in each group with tank duplicates ($n = 8$ per tank). To develop Mn-induced Parkinsonism, we chose 2 mM of Mn and exposure duration of 21 days, based on a previously published method (Nadig et al., 2022). Mn-exposure water was renewed daily. Vehicle was injected into control fish, whenever test fish were injected with either DZ or Don. DZ dosages of 10, 20, and 40 mg·kg⁻¹ (DZ1, DZ2, and DZ3 respectively) were chosen based on the MTD in a pilot acute toxicity study. After the experimental period, fish from each group were randomly tested for cognitive function. To minimize the experimental animals, we have adopted a test battery approach (Song et al., 2016). After behavioural recordings, zebrafish were killed immediately by a two-step procedure involving i) general anaesthesia using buffered MS222 (200 mg·L⁻¹) until the loss of motor coordination, ii) followed immediately by hypothermic shock (2–4°C) to minimize the physiological and psychological stress. The death of zebrafish was confirmed by the cessation of opercular movements, as suggested by ARAC Guidelines. After the test battery, brains were dissected carefully under a dissection microscope and either stored at –80°C for further biochemical/molecular analysis or immediately fixed and processed for histopathological analysis.

2.6 | Behavioural recordings

All the behavioural recordings were conducted in an isolated noise-free room at 27 ± 1°C, and the zebrafish were acclimatized to the behavioural recording room for 1 h before the video recording. Behavioural recordings were performed between 0900 and 1500 to avoid hormone-associated behavioural disturbances. We have used an integrated recording platform, as mentioned in our previous study (Haridevamuthu et al., 2024). It consists of Sony CMOS IMX586 1/2.0" 48 MP sensor connected to OnePlus Camera software (Ver. 7.0.50, AC2001, OnePlus Technology Co., Ltd., India) and mounted on a stable tripod. The platform is remotely controlled to avoid unnecessary psychological disturbances. Video resolution was 1920 × 1080 pixels (1080p) with a frame rate of 30 frames per second. After each experiment, the videos were transferred to a computer as an MP4 file without

TABLE 1 Animal experiment grouping and dosing regimen. Tank duplicate for each group with eight animal per tank was maintained.

Grouping	Description	Administration details	Route of administration	Number of animal
VC	Vehicle control	1% DMSO in 0.9% sterile saline solution	<i>i.p.</i> at 7th and 14th day	$n = 16$
MnCl ₂	PD model	2 mM of manganese chloride	Water exposure from 0th to 21st day	$n = 16$
Don	Standard drug	4 mg·kg ⁻¹ b.w. of donepezil hydrochloride	<i>i.p.</i> at 7th and 14th day	$n = 16$
DZ1	Daidzein intervention	10 mg·kg ⁻¹ b.w. of daidzein	<i>i.p.</i> at 7th and 14th day	$n = 16$
DZ2		20 mg·kg ⁻¹ b.w. of daidzein	<i>i.p.</i> at 7th and 14th day	$n = 16$
DZ3		40 mg·kg ⁻¹ b.w. of daidzein	<i>i.p.</i> at 7th and 14th day	$n = 16$

compression. Illumination was provided by a flicker-controlled 350 luminous LED lamp wrapped in white vellum paper. To minimize the tank effect, we reassigned each experimental group between recordings. Swimming coordinates were generated by UMATracker (<http://ymnk13.github.io/UMATracker/>) (Yamanaka & Takeuchi, 2018).

2.7 | Novel tank diving test

Locomotor activity and anxiety behaviour of the test fish were evaluated by the novel tank diving test (Haridevamuthu, Raj, et al., 2023). An acrylic tank (21.5 cm × 11.5 cm × 22.5 cm) with 4.5 L of water filled up to 18.2 cm was used. The tank was pasted with white cellophane paper on three sides, and illumination was provided from the back of the tank. Video recording by the lateral view was started immediately after the test fish were introduced into the novel tank and continued for 6 min. Anxiety endpoints, such as time spent in the top area and latency to reach the top area, were evaluated by an experienced observer blinded to the experiment (interrater reliability >0.85) (Faria et al., 2018).

2.8 | Light–dark test

Scototaxis of test fish were assessed by the light–dark test (Maximino et al., 2018; Mezzomo et al., 2016). An acrylic tank (21.5 cm × 11.5 cm × 22.5 cm) was equally divided into light and dark regions by covering it with black and white cellophane papers. Illumination was provided from two sides of the tank. Video recording by the dorsal view was started immediately after the test fish were introduced into the light–dark tank and continued for 6 min. Scototaxis endpoints such as time spent in the light region, shuttling between the light and dark regions, and latency to enter the light region were evaluated by an experienced observer blinded to the experiment (interrater reliability >0.85).

2.9 | Olfactory preference test

The olfactory function of test fish was assessed by an olfactory preference test using a mixture of amino acids as olfaction stimuli (Koide et al., 2009; Nadig et al., 2022). Briefly, the test fish were placed in the experimental tank (21.5 cm × 11.5 cm × 22.5 cm) and habituated for 10 min. Intravenous fluid infusion set with flow regulator was used to deliver stimuli at a rate of 1.5 ml·min^{−1} into a corner of the tank. Fish water was delivered for 2 min as pre-stimulation and, quickly, amino acid mixture (0.1 mM of Cys and Met) was switched for 2 min. Video recording was started at prestimulation, and olfactory preference endpoints, such as time spent in the amino acid region (TAA) and time spent in the non-amino acid region (TNAA), were evaluated by an experienced observer blinded to the experiment (interrater reliability > 0.85). Preference index was calculated using Equation (1).

$$\text{Preference Index} = (TAA - TNAA) / (TAA + TNAA) \times 100 \quad (1)$$

2.10 | Conspecific preference test

The interactive behaviour of test fish was assessed by a conspecific preference test using live zebrafish conspecifics (Boopathi et al., 2024). An experimental tank (21.5 cm × 11.5 cm × 22.5 cm) with three chambers divided by transparent glass was used. Naïve zebrafish conspecifics were introduced in one end of the chamber and named as the conspecific tank (CT). The other end was left empty and named as the empty tank (ET). The test fish were introduced into the middle chamber which was named as the middle tank. The middle tank was further virtually divided into three zones: empty zone (E), middle zone (M), and conspecific zone (C). Initially, the transparent glass was covered by an opaque lid, and test fish were habituated in the middle tank for 5 min. After habituation, the opaque lids were removed and test fish movement towards the zones were recorded for 5 min. Social interaction endpoints, such as time spent in the conspecific zone and empty zone, were evaluated by an experienced observer blinded to the experiment (interrater reliability >0.85).

2.11 | Shoaling test

Anxiety of test fish can be measured by their shoaling behaviour (Pham et al., 2012). Shoaling is an adaptive behaviour with organized swimming movements that is impacted by environmental and pharmacological stressors. An acrylic tank (21.5 cm × 11.5 cm × 22.5 cm) with 4.5 L of water filled up to 18.2 cm was used. Five fish from the experimental group were randomly introduced into the tank and left to adapt to the tank for 5 min. This acclimatization to novel tank reduced transfer anxiety and re-established their natural shoaling behaviour (Pham et al., 2012). Video recording at the lateral view was started after the test fish acclimatization period and continued for 3 min. Videos were then postprocessed in Microsoft Photos software and still pictures were captured every 15 s from the 3 min video (12 images per group). The images were calibrated, and endpoints such as nearest fish distance (cm), farthest fish distance (cm), and shoal area (cm²) were measured using Fiji software (Ver. 1.53t).

2.12 | Biochemical assays

Following behavioural recordings, test fish were sacrificed immediately by a two-step procedure involving general anaesthesia using buffered MS222 (200 mg·L^{−1}) until the loss of motor coordination, followed immediately by hypothermic shock (2–4°C). The entire brain was carefully excised by opening the skull and removing bone residues from both the dorsal and ventral sides of the brain, in

accordance with the standard dissection protocol (Gupta & Mullins, 2010). Isolated whole brain tissues were subsequently rinsed with ice-cold PBS and promptly processed for biochemical analysis. Whole brain tissues ($n = 6$ per group) (including olfactory bulb, cerebrum, tectum, cerebellum, and medulla) were individually homogenized (65% amplitude, 15-s pulses with 10-s intervals for a total of 90 s) in 100-mM ice-cold phosphate buffer (pH 7.4) using an Vibracell homogenizer (VCX 130, Newtown, CT) under ice, each serving as a biological replicate. The homogenate were centrifuged at 800g for 10 min at 4°C, and the resultant supernatant was either stored at –80°C or utilized for further analysis. Acetylcholinesterase (AChE) activity was assessed by Ellman's method (Ellman et al., 1961). Superoxide dismutase (SOD) and **catalase** (CAT) activities were determined using the pyrogallol auto-oxidation (Marklund & Marklund, 1974) and **hydrogen peroxide** consumption methods (Ellerby & Bredesen, 2000), respectively. Reduced **glutathione** (GSH) levels and glutathione peroxidase (GPx) specific activity were assayed by the DTNB (5,5'-dithiobis-2-nitrobenzoic acid) reaction (Ganie et al., 2011). Lipid peroxidation was evaluated by measuring malondialdehyde (MDA) levels, using the TBARS (thio-barbituric acid reactive substance) method (Ohkawa et al., 1979). Reactive species formation was assessed using the dichlorodihydro-fluorescein diacetate (DCFH-DA) method (de Sá-Nakanishi et al., 2014). Protein quantification was performed using Bradford's method (Bradford, 1976).

2.13 | Histological alterations

Whole brains ($n = 5$ per group) were excised and fixed in 10% buffered **formalin** for 24 h at 4°C. Subsequently, the fixed brains underwent dehydration with a gradient of ethanol, followed by xylene, and were then embedded in paraffin wax for sectioning. The paraffin wax blocks were sliced into horizontal sections with a thickness of 8–10 μm using a rotary microtome (Leica R125 RM). The sections were dewaxed using xylene and rehydrated with a gradient of ethanol as described previously (Haridevamuthu, Raj, et al., 2023). Following preparation, the sections were stained with haematoxylin-eosin (H&E) and examined under an EXC-500 upright microscope (Accu-Scope®, NY, USA). Images of tectum opticum were captured using a mounted Excelis MPX-5C Pro camera connected to CaptaVision+™ PC imaging software (Ver. 2.4.1) via USB 3.0 cable. The regions were identified based on the zebrafish brain topological atlas (Wullmann et al., 1996). Histopathological alterations, including glial cell morphology, myelinated axons, pyknosis, vacuolization, and immune cells, were assessed on each slide using a semiquantitative scoring system: +++, severe histopathological alteration; ++, moderate histopathological alteration; +, mild histopathological alteration; –, no histopathological alterations (Haridevamuthu, Raj, et al., 2023). The scoring was conducted by experienced pathologists who were blinded to the experimental conditions. The grades from all slides were averaged to determine the final grade for each individual test fish.

2.14 | Detection of dopamine and DOPAC

Isolated whole brains ($n = 5$ per group) (including olfactory bulb, cerebrum, tectum, cerebellum, and medulla) were washed with ultrapure water and immediately homogenized under liquid nitrogen. The homogenate was suspended in ice-cold methanol and centrifuged at 5000g for 15 min at 4°C. The resulting supernatant were filtered using 0.2- μm PTFE Corning® syringe filters (Corning Inc., NY, USA) and stored in GC vials under –80°C until HPLC analysis. DA and DOPAC from the filtered brain homogenate were directly injected into an Agilent 1220 Infinity II LC System (Agilent Technologies, Inc., Santa Clara, USA) with an injection volume of 10 μl . ZORBAX StableBond C18 (4.6 \times 150 mm, 5 μm) at 35°C was used for separation and eluted using methanol and acetonitrile (70:30) with a flow rate of 1 $\text{ml}\cdot\text{min}^{-1}$ and a UV-PDA detector set at 280 nm. The quantitative analysis was conducted by comparing the DA and DOPAC standard dissolved in HPLC grade methanol at concentrations of 2, 4, 6, 8, and 10 $\mu\text{g}\cdot\text{ml}^{-1}$.

2.15 | Data and statistical analysis

The data in this study, including behavioural video files, were processed using a Dell OptiPlex 3070 MT Desktop PC (Dell Inc., India) equipped with a 9th Gen 3.6 GHz Intel i3-9100 CPU Quad-core processor integrated with Intel UHD Graphics 630. The desktop computer was configured with 8 GB DDR4 RAM and operated on the Windows 11 Pro operating system ($\times 64$). Graphing and statistical analyses were performed using GraphPad Prism software (Ver 9, GraphPad Software Inc., San Diego, USA) (www.graphpad.com) (RRID: SCR_002798). Locomotion trajectories were plotted using OriginPro software (Ver 2019b, OriginLab Corporation, USA) (RRID: SCR_014212). All the software used in this study was built for Windows OS ($\times 64$). Data are presented as mean \pm SD of biological replicates. The Kaplan–Meier survival graph was generated for DZ acute toxicity, and the Log-rank (Mantel–Cox) test was employed for curve comparison. Assuming a Gaussian distribution, ordinary one-way analysis of variance (ANOVA) was applied to all data where each group size was at least $n = 5$. A family-wise alpha threshold of 0.01 was considered statistically significant with a 99% confidence interval. If $P < 0.01$ in ANOVA, a post hoc Dunnett's multiple comparison test was employed to identify the statistical difference between the mean of each column and the mean of MnCl_2 column. The normality of the data was verified using the Shapiro–Wilk test, and clustering was assessed using Bartlett's test. The group size in this study is the number of independent values (not technical replicates), and that statistical analysis was done using these independent values. Data and statistical analyses comply with the recommendations of the *British Journal of Pharmacology* on experimental design and analysis (Curtis et al., 2023).

2.16 | Nomenclature of Targets and Ligands

Key protein targets and ligands in this article are hyperlinked to corresponding entries in <https://www.guidetopharmacology.org>, and are

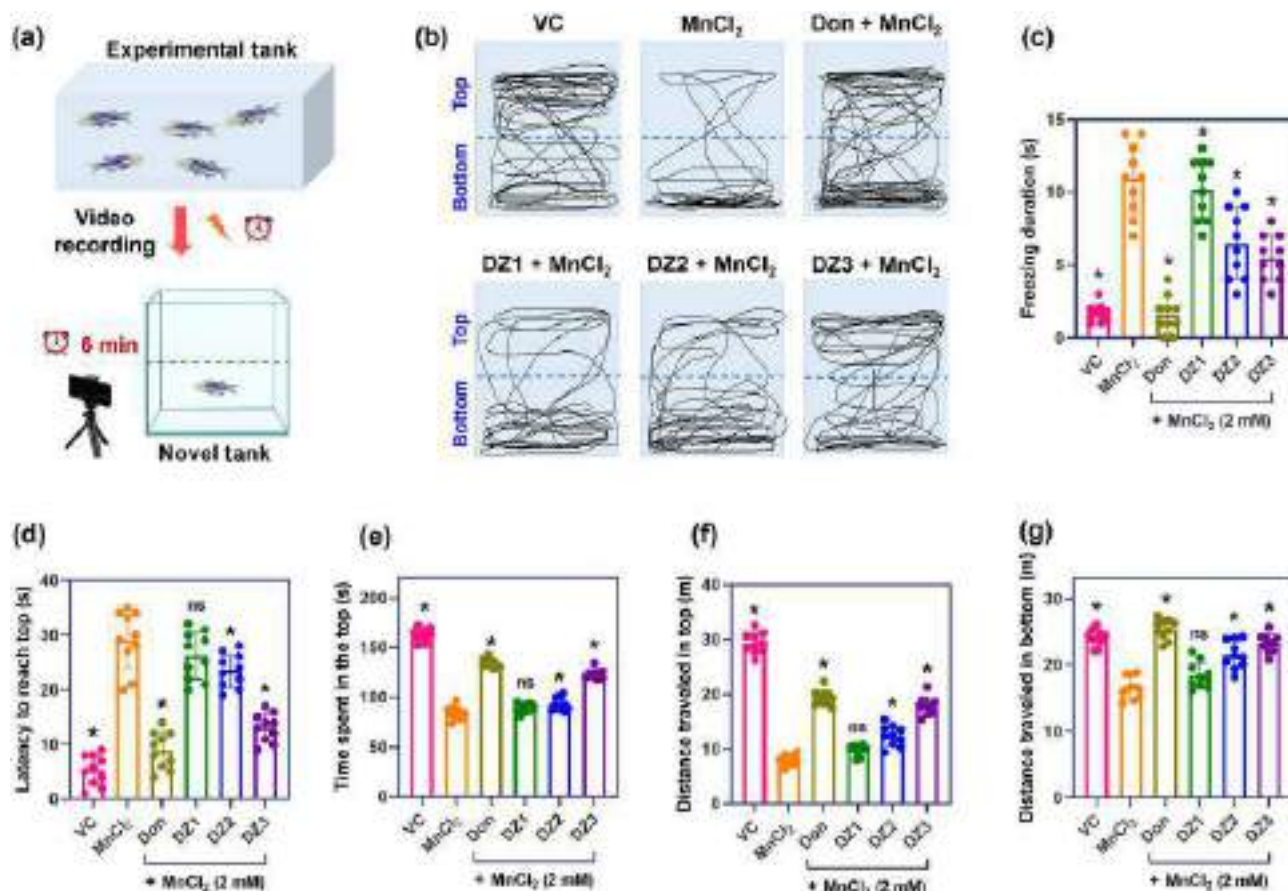


FIGURE 2 (a) Recording setup for novel tank test. (b) Locomotion trajectories of test zebrafish in novel tank after receiving various administrations, (c) freezing duration of the test fish in novel tank. (d) latency to reach the top region (s), (e) time spent in the top region (s), (f) total distance travelled in the top (m), and (g) total distance travelled in the bottom (m) of the test fish in novel tank. Data were expressed as mean \pm SD of biological replicates ($n = 10$). * $P < 0.01$, ns—not significant compared with the MnCl₂ group.

permanently archived in the Concise Guide to PHARMACOLOGY 2023/24 (Alexander et al., 2023).

3 | RESULTS

3.1 | DZ improved motor ability and bradykinesia in Mn-induced Parkinsonism

The behaviour pattern of the test fish, recorded immediately after being introduced into a novel tank, was assessed to determine the anxiolytic effect of DZ on Mn-induced Parkinsonism (Figure 2a). The locomotion was plotted to represent the test fish trajectory inside the novel tank (Figure 2b). It shows that Mn-induced anxiety is recorded by increased movement at the bottom of the tank when compared with VC (vehicle control). Freezing time was significantly increased in Mn-exposure and reduced by DZ intervention with a higher reduction at the 40 mg·kg⁻¹ dose (Figure 2c). Latency to reach the top region (Figure 2d), time spent in the top region (Figure 2e), and distance travelled in top (Figure 2f) were significantly reduced with Mn-exposure when compared with VC. In contrast, distance travelled in the bottom (Figure 2g) was increased

with Mn-exposure. Latency, time spent, and distance travelled at the top by the test fish were significantly increased with the administration of Don and DZ3 (40 mg·kg⁻¹) group when compared with the MnCl₂ group. We also observed bradykinesia-like symptoms in Mn-exposed fish. This was evident by the significant reduction in total swimming distance. Total distance was significantly restored by Don, DZ2 (20 mg·kg⁻¹), and DZ3 (40 mg·kg⁻¹) when compared with the MnCl₂ group. Bradykinesia is a prominent clinical manifestation of PD, which was improved by DZ intervention. In contrast, DZ at 10 mg·kg⁻¹ dose (DZ1) did not have any effect on freezing duration, latency, time spent in the top, and distance travelled in the top and bottom.

3.2 | DZ reduces anxiety-like symptoms in Mn-induced Parkinsonism

The anxiety-like symptoms exert by the test fish were recorded with the light-dark test and shoaling behaviour and assessed to determine the anxiolytic effect of DZ on Mn-induced Parkinsonism. Mn-exposed fish spent significantly less time in light region (Figure 3a) and shuttling between regions (Figure 3b) also were

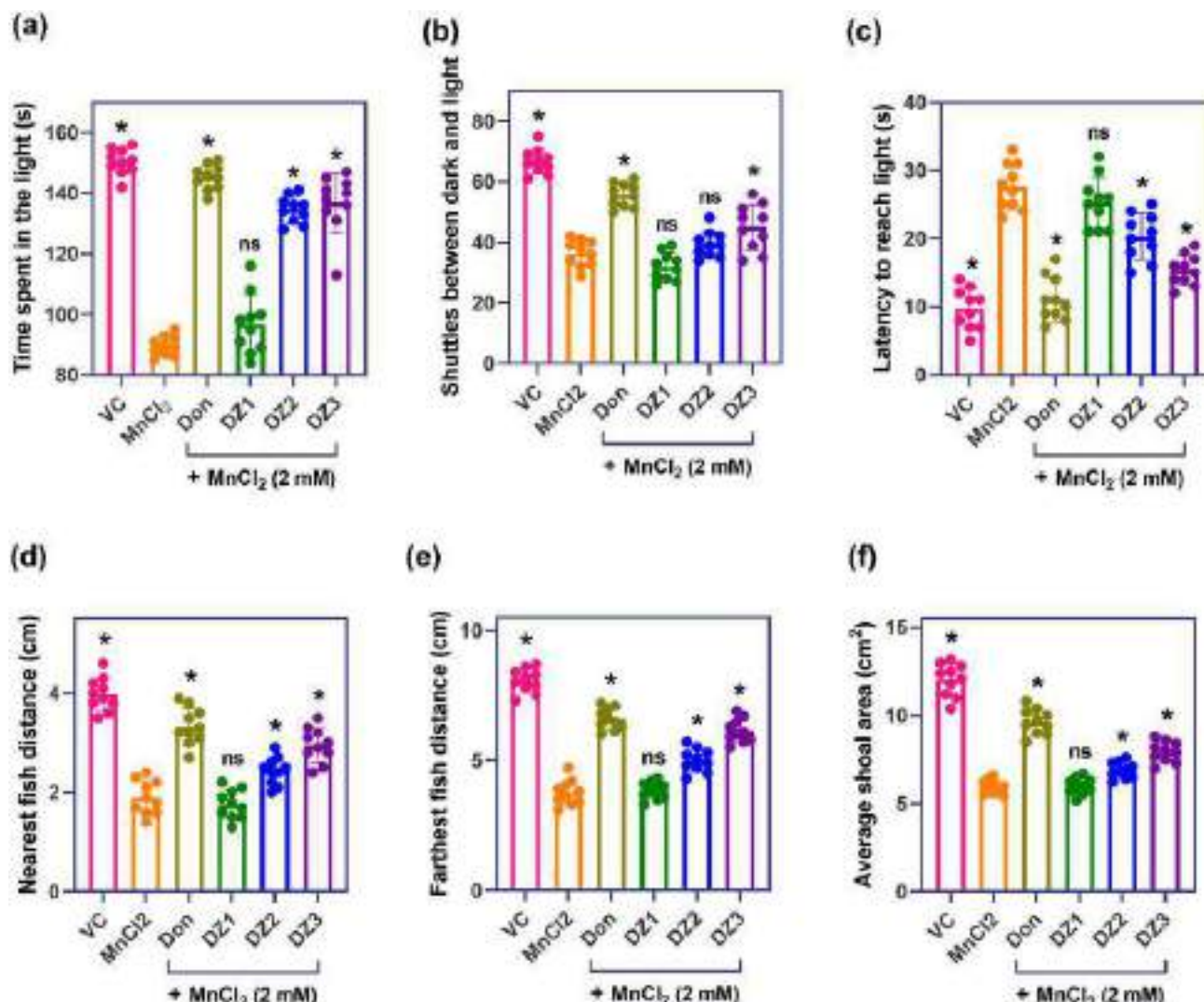


FIGURE 3 (a) Time spent in the light region (s), (b) number of shuttling between the dark and light region, and (c) latency of the fish to reach the light region (s) in the light and dark box setup. (d) Nearest neighbouring fish distance (cm), (e) farthest neighbouring fish distance (cm), and (f) average shoal area (cm²) of the test fish in shoaling assay. Data were expressed as mean \pm SD of biological replicates ($n = 10$). * $P < 0.01$, ns—not significant compared with the MnCl₂ group.

reduced when compared with VC fish. The latency to enter the light region was higher in Mn-exposed fish than VC fish in the light and dark box (Figure 3c). Mn-induced tight shoaling behaviour as evident by the significant decrease in nearest and farthest fish distance (Figure 3d,e) resulting in decreased shoal area (Figure 3f) when compared with VC. This indicates that Mn-exposed fish experience anxiety-like symptoms. Time spent in the light and shuttling between the regions were significantly increased in fish intervened with Don and DZ3 (40 mg·kg⁻¹). Don and DZ3 (40 mg·kg⁻¹) reduces the time taken for the fish to reach the light when compared with the MnCl₂ group, implying that DZ reduces the anxiety-like behaviour in Mn-induced Parkinsonism. In contrast, DZ at 10 and 20 mg·kg⁻¹ dose did not have any effect on shuttling between the region, latency to reach the light region, nearest fish distance, and shoal area.

3.3 | DZ improves olfactory function in Mn-induced Parkinsonism

Olfactory function of the test fish was assessed by amino acid stimuli to create an odour rich zone (Figure 4a). The schematic diagram of the olfactory preference experiment was shown in Figure 4b. The test fish locomotion was recorded from 2 min of pre-stimulation and continued for 3 min after odour stimulation. The locomotor trajectories show that healthy VC fish moved towards amino acid zone where Mn-induced fish did not (Figure 4c). The test fish preference towards amino acid and non-amino acid zone was calculated by preference index and found that Mn-exposed fish showed lesser preference towards amino acid zone when compared with VC. Time spent in the amino acid zone also was lower in Mn-exposed fish than VC fish. These preference indices further provided evidence that Mn-exposure

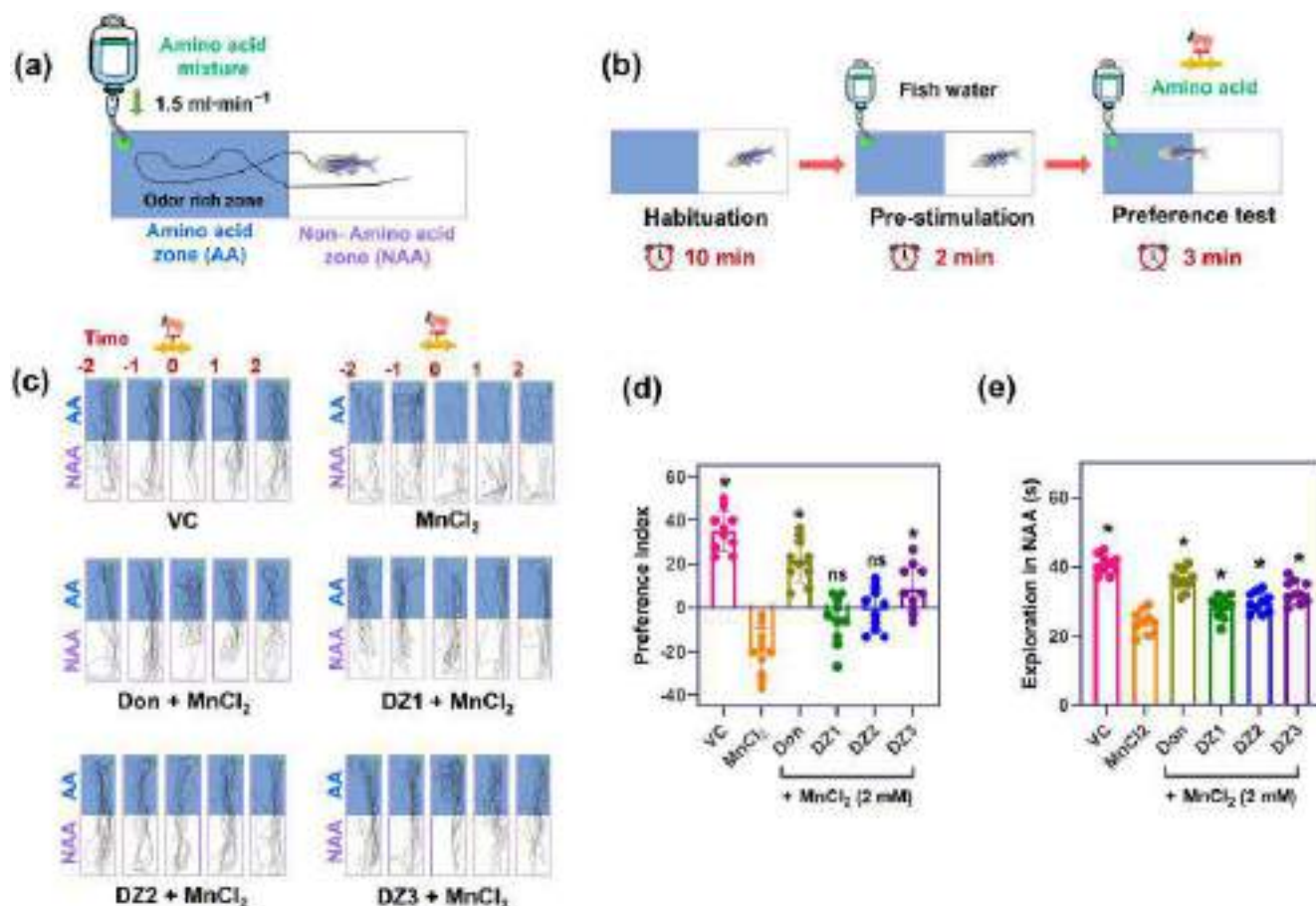


FIGURE 4 Schematic representation of (a). Olfactory preference test setup. (b) Prestimulation and amino acid stimuli test. (c) Locomotion trajectories of test fish before and after amino acid stimuli. (d) Preference index of test fish towards amino acid rich zone. (e) Exploration time in the NAA (s). TAA—time spent in amino acid zone and TNAA—time spent in non-amino acid zone. Data were expressed as mean \pm SD of biological replicates ($n = 10$). * $P < 0.01$, ns—not significant compared with the MnCl₂ group.

causes olfactory dysfunction. Don and DZ3 (40 mg·kg⁻¹) significantly increased the fish preference index towards amino acid stimuli and increased the time spent in the amino acid zone when compared with the Mn-exposed group. Intervention with Don and DZ improved olfactory response to amino acid stimuli as evident from the trajectories.

3.4 | DZ recovers social behaviour in Mn-induced Parkinsonism

Social preference of the test fish was assessed by live conspecific stimuli at one end of the conspecific tank (Figure 5a). The schematic diagram of the social preference experiment was shown in Figure 5b. The test fish locomotion in conspecific tank was recorded for 5 min. From the trajectory plots, it is visualized that VC fish leaves more trajectory near conspecific region, whereas Mn-exposed fish swam across the tank (Figure 5c). Time spent in the conspecific region was reduced significantly in Mn-exposed fish when compared with VC (Figure 5d). In contrast, time spent in the empty region was

increased in Mn-exposed fish than VC (Figure 5e). Don, DZ2 (20 mg·kg⁻¹), and DZ3 (40 mg·kg⁻¹) significantly increases the time spent in the conspecific region and decreases the amount of time spent in the empty region when compared with the Mn-exposed group. Intervention with Don and DZ recovers the social behaviour of test fish to live conspecific stimuli as evident from their trajectories.

3.5 | DZ reduces brain oxidative damage in Mn-induced Parkinsonism

Mn-exposure significantly reduced the hydrogen peroxide scavenging enzyme CAT (Figure 6a) and GSH levels (Figure 6b) in brain tissue when compared with VC fish. Furthermore, Mn-exposure significantly increased MDA levels (Figure 6c), reactive species formation (Figure 6d) and decreased cell viability (Figure 6e) of brain tissue when compared with VC fish brain. Mn also increased the AChE activity compared with VC, which may lead to motor neuron dysfunction (Figure 6f). Alternatively, Don and DZ3 (40 mg·kg⁻¹)

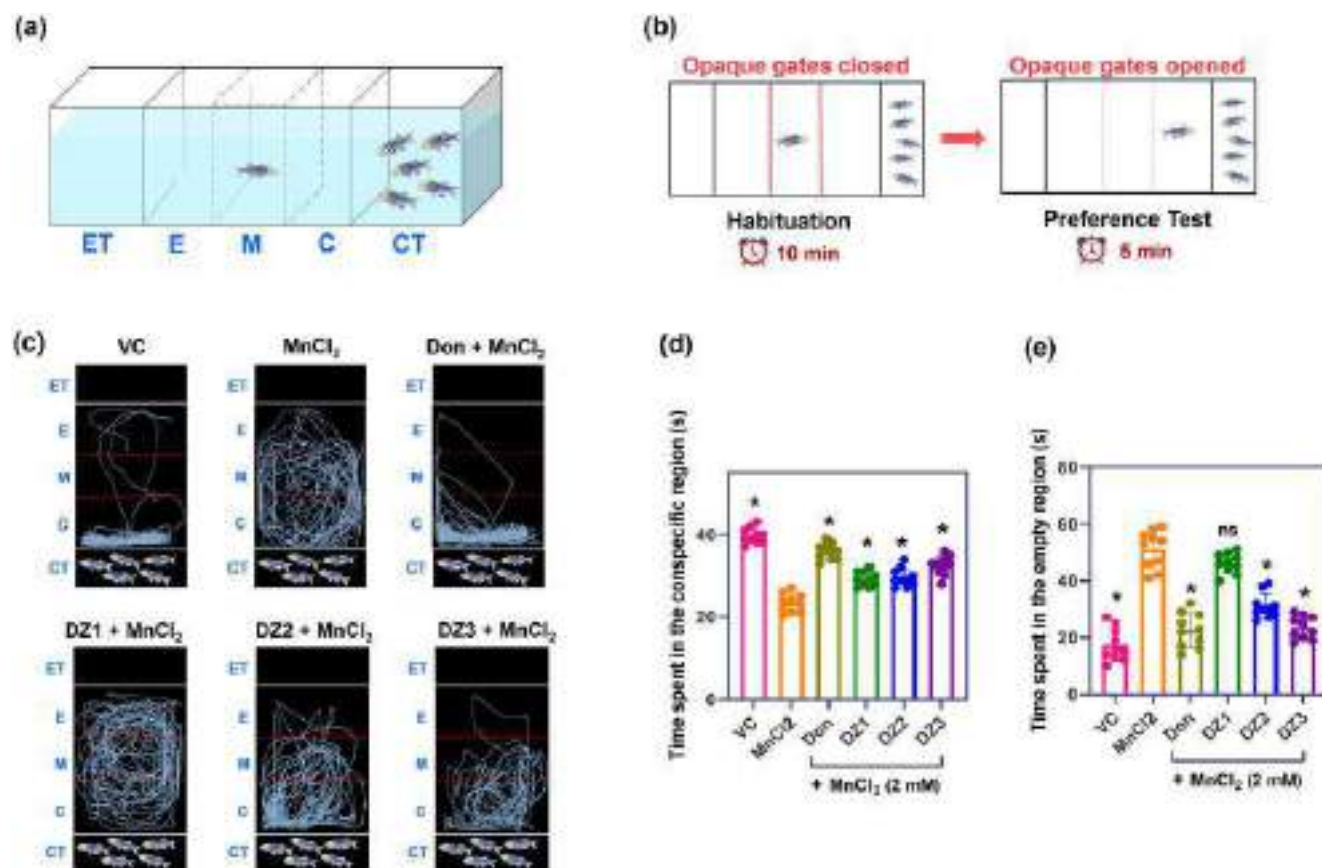


FIGURE 5 Schematic representation of (a) social preference test setup, (b) habituation to the setup and live conspecific stimuli test, (c) locomotion trajectories of test fish during live conspecific stimuli, (d) time spent in the conspecific region (s) and (e) time spent in the empty region (s) by test fish inside social preference tank. ET—empty tank, E—empty zone, M, middle zone, C, conspecific zone, and CT—conspecific tank. Data were expressed as mean \pm SD of biological replicates ($n = 10$). * $P < 0.01$, ns—not significant compared with the MnCl₂ group.

administration increased the CAT activity and GSH levels in brain compared with MnCl₂ fish. Don and DZ3 (40 mg·kg⁻¹) also significantly reduced MDA levels, reactive species formation, and increased the overall cell viability of fish brain. AChE activity was reduced by Don and DZ3 (40 mg·kg⁻¹). These biochemical results indicate that DZ reduces the brain oxidative damage caused by Mn.

3.6 | DZ prevents brain histopathological alterations in Mn-induced Parkinsonism

Histological sections of tectum opticum indicated that VC brain had undamaged cellular morphology with distinct oligodendroglia cells and myelinated axons (Figure 7a). Mn-exposed tectum opticum clearly showed severe cellular damage, with less glial cells and myelinated axons. Pyknosis, vacuolization of glial cells, and immune cell infiltration were higher in Mn-exposed brains. The severity level of pyknosis, vacuolization, and immune cells was mild in Don and DZ3 (40 mg·kg⁻¹) interventions. Don and DZ3 administration rescued the distinct neuronal morphology of Mn-induced Parkinsonism. The

semiquantitative ordinal scoring for histological alteration was performed as described before in Table 2. This histological alteration was associated with the oxidative stress induced by Mn in brain regions.

3.7 | DZ increases dopamine level in Mn-induced Parkinsonism

We have chosen the DZ3 (40 mg·kg⁻¹) dose for the dopamine analysis and eliminated the DZ1 and DZ2 groups because they did not show significant results on behavioural and biochemical tests. Dopamine (DA) and its metabolite 3,4-dihydroxyphenylacetic acid (DOPAC) was estimated from the whole brain tissue (including olfactory bulb, cerebrum, tectum, cerebellum, and medulla) of the test fish to evaluate the function of dopaminergic neurons. Mn-exposed fish showed a lower level of DA (Figure 7b) and a higher level of DOPAC (Figure 7c) in the brain tissue when compared with VC fish. The DOPAC/DA ratio (Figure 7d) also was higher in Mn-exposure group, reflecting the higher DA level. Intervention with Don and DZ3 (40 mg·kg⁻¹) significantly increases the DA and lowers the DOPAC levels in brain tissue, thus reducing the DOPAC/DA ratio when compared with MnCl₂ fish.

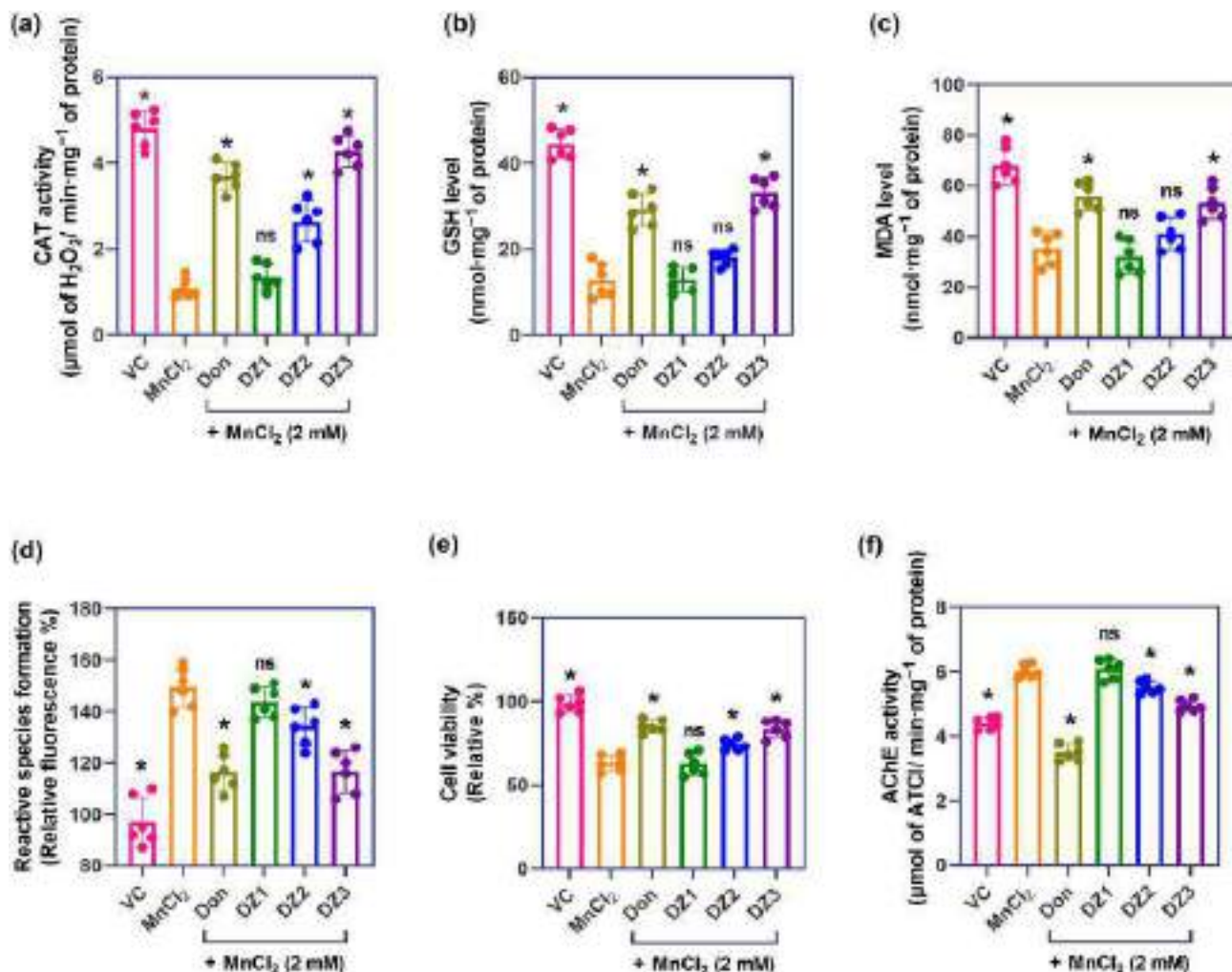


FIGURE 6 (a) CAT activity ($\mu\text{mol of H}_2\text{O}_2/\text{min}/\text{mg}$ of protein). (b) GSH level ($\text{nmol}\cdot\text{mg}^{-1}$ of protein). (c) MDA level ($\text{nmol}\cdot\text{mg}^{-1}$ of protein). (d) Reactive species formation (relative fluorescence %). (e) Relative cell viability (%) and (f) AChE activity ($\mu\text{mol of ATCl}/\text{min}/\text{mg}$ of protein) in whole brains tissues of different experimental groups. Data were expressed as mean \pm SD of biological replicates ($n = 6$). * $P < 0.01$, ns—not significant compared with the MnCl_2 group.

4 | DISCUSSION

Manganese (Mn) is a vital micronutrient necessary for normal cellular development and growth (Kwakye et al., 2015). It is found at low concentrations in legumes, pineapples, beans, nuts, tea, and grains (Harischandra et al., 2019). Under physiological conditions, Mn serves as an essential cofactor for various enzymes, including pyruvate decarboxylase, glutamine synthetase, manganese-superoxide dismutase (Mn-SOD), and arginase, which are crucial for neurotransmitter synthesis and metabolism, as well as for the functionality of neurons and glial cells (Erikson & Aschner, 2003; Kwakye et al., 2015). Despite its nutritional benefits, excessive exposure to Mn during prenatal and postnatal periods can adversely impact on infant neurodevelopment and has been linked to impaired cognition and motor coordination resembling PD (Claus Henn et al., 2010). Besides motor dysfunction, clinical studies suggest that Mn causes nonmotor symptoms such as anxiety, depression, olfactory dysfunction, and social dysfunction

(Racette et al., 2021). Marketed clinical drugs are primarily focused on motor symptoms, whereas nonmotor symptoms typically are neglected. Therefore, we have performed neurobehavioural analyses in adult zebrafish to evaluate the role of DZ in improving the nonmotor symptoms.

Ceruloplasmin oxidizes the Mn^{2+} valance state to Mn^{3+} and is localized in neuronal endosomes via the **transferrin receptor (CD71) / divalent metal transporter 1 (DMT1)** complex (Harischandra et al., 2019). Mn^{3+} dissociates from endosomes during **v-ATPase** acidification and reduces to Mn^{2+} , which is stable in physiological pH, accounting for Mn deposition in basal ganglia (Harischandra et al., 2019). Mn^{2+} primarily accumulates in mitochondria, where it inhibits the activity of complex I/II and **F1ATPase**, leading to interference with Ca^{2+} -activated **ATP** production. This inhibition results in the loss of mitochondrial potential, triggering oxidative stress as seen in this study (Tarale et al., 2016). DMT1 expresses highly in dopaminergic neurons, leaving dopamine particularly susceptible to Mn

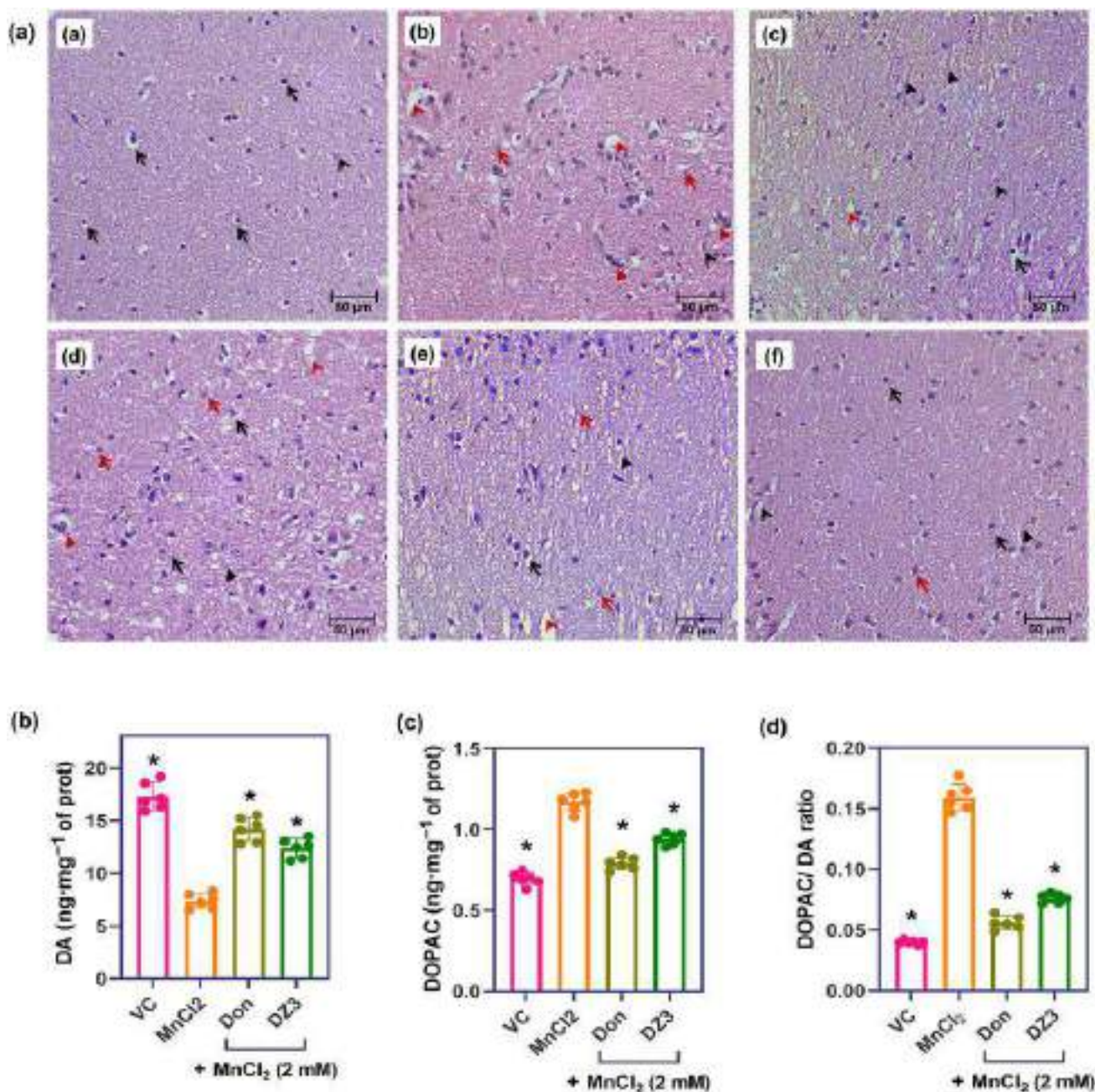


FIGURE 7 (a) Histopathological alteration caused by Mn in tectum opticum region of zebrafish brain of different experimental groups, (A) VC, (B) MnCl₂, (C) Don, (D) DZ1, (E) DZ2, and (F) DZ3. Black open arrow—glial cell; black open arrow head—capillary; black arrow head—myelinated axons; red open arrow—pyknosis; red open arrow head—vacuolization; red arrow head—immune cells. Magnification—400 \times . Scale—50 μm . (b) DA level ($\text{ng}\cdot\text{mg}^{-1}$ of protein), (c) DOPAC level ($\text{ng}\cdot\text{mg}^{-1}$ of protein), and (d) DOPAC/DA ratio present in in whole brains tissues of different experimental groups. Data were expressed as mean \pm SD of biological replicates ($n = 5$). * $P < 0.01$, ns—not significant compared with the MnCl₂ group.

attack. Mn also has been reported to promote dopamine oxidation in dopaminergic neurons, leading to an increase in the production of o-quinone, aminochrome, and 5,6-indolequinone (Ávila et al., 2021). Dopamine oxidation might be responsible for the reduction of the available dopamine in brain regions and would create an imbalance between DA and DOPAC, as evident from this study. This imbalance affects dopamine neurotransmission, which is reflected by reduced motor movements of zebrafish in this study. Mn²⁺ also

catalyses the conversion of H₂O₂ to the hydroxyl radical ($\cdot\text{OH}$) through the Fenton reaction, and lead to severe oxidative stress. This process contributes to the generation of excessive reactive oxygen species (ROS) (Nadig et al., 2022). The produced free radicals induce structural and functional modifications of antioxidant proteins (Tinkov et al., 2021). The impairment of the cellular antioxidant machinery, leading to an imbalance between the generation and elimination of ROS, is a crucial factor in the progression of neurodegeneration. The

TABLE 2 Semi-quantitative histological scoring of zebrafish brains of Mn-induced parkinsonism. (–, no alterations; + mild alterations; ++, moderate alterations/damage; +++, severe alterations/damage).

Grouping	Histological alterations				
	Glial cell morphology	Myelinated axons	Pyknosis	Vacuolization	Immune cells
VC	+++	+++	–	–	–
MnCl ₂	+	–	+++	+++	++
Don	++	++	+	++	–
DZ1	+	–	+++	+++	++
DZ2	+	+	++	+++	+
DZ3	++	++	+	+	–

antioxidants, CAT and GSH, found in neurons and astrocytes, serves as the initial line of cellular defence against ROS. CAT hydrolyses the H₂O₂ produced by Mn²⁺ into water and oxygen, whereas GSH actively eliminates exogenous peroxides by participating as a co-substrate in reactions catalysed by GPx, thereby playing crucial functional roles in the central nervous system (CNS). Disturbances in the concentrations of GSH and MDA and the activities of CAT and GPx have been previously observed in association with Mn-induced neurotoxicity (manganism) (Nkpaa et al., 2022). This suggests that an impaired neuronal antioxidant system renders the brain susceptible to manganism. Isoflavones such as DZ, formononetin, and irilone from red clover and soy can improve dopamine levels and reduce dopaminergic neuronal loss caused by xenobiotics. It is already evident from many studies that DZ is a ROS quencher and capable of improving antioxidant defence (Alshehri et al., 2021; Guru et al., 2022; Li et al., 2021). This study further provides evidence that DZ could improve dopamine levels and maintain antioxidant status in Mn-exposed brain.

Mn is known to impact the homeostasis of various neurotransmitter systems, particularly the cholinergic system, as documented in previous studies (Anjum et al., 2019; Ferreira et al., 2022). The cholinergic components have been recognized for their modulatory role in learning, memory, and motor processes, which also are affected by manganism (Ferreira et al., 2022). In this study, the activity of AChE in the brain was investigated to determine whether DZ restores the cholinergic system affected by chronic Mn exposure. The results indicated that the DZ reduces the AChE activity in the brain and exerts AChE inhibitor activity, similar to donepezil. This aligns with previous findings that DZ decreases the brain AChE activity of ovariectomy-induced cognitive-deficit rats (Jaiswal et al., 2023). Moreover, recently DZ-derived synthetic analogues have been designed and tested for their inhibition activity on AChE enzyme (Y. Wang et al., 2023). These deleterious effects significantly reduced the viable cells, verified by MTT assay. Due to increased antioxidant status in the brain by intervention of DZ, brain cell viability was enhanced, which reflects the histopathological and behavioural findings in the current study. Histological analysis further provides evidence to the cellular protection resulting from DZ treatment. Mn-exposed brains showed destructured cellular morphology without rigid structure. The migration of immune cells in the brain

tissue indicates inflammation and toxic invasion. Pyknotic bodies were clearly seen, indicating oxidative brain injury. Prolonged Mn exposure caused vacuolization in glial cells, which indicates a neurodegeneration process resembling the pathology of PD. The loss of neurons and glial cells is strongly correlated with the chronic oxidative stress exerted by Mn. DZ intervention could be used to partially recover the cellular damage. The increase in antioxidant status of the DZ-intervened brain was reflected in its distinct cellular morphology.

In investigating the effects of Mn-induced Parkinsonism, particularly in terms of motor impairments, the study initially focused on analysing the locomotor and exploratory behaviour of test fish exposed to Mn over a period of 21 days. The novel tank test was employed, a contextually relevant assay based on the instinct of animals to seek protection in an unacquainted environment, typically expressed through behaviours such as diving, freezing, and reduced exploration (Ferreira et al., 2022). Mn-exposed fish spent more time in the bottom region with reduced exploration, which reflects anxiety-like symptoms. The findings from this study align with previous findings in both larvae and adult zebrafish exposed to Mn exhibiting locomotor deficits (Altenhofen et al., 2017). Mn also reduced the time spent in the light region and shuttling. As a behavioural endpoint, risk assessment of animals is linked to the defensive approach, involving a meticulous exploration of potentially aversive environments (Kalueff et al., 2013). The emergence of these phenotypes signifies heightened anxiety-like behaviour and a defensive approach. Given that anxiety can reduce social behaviour, the study also examined the impact of Mn on the intrasocial and intersocial behaviour. This test reflects the innate inclination of fish to form shoals and where individuals seek the presence of conspecifics (Miller & Gerlai, 2007). We found that Mn-exposed zebrafish exhibited anxiety episodes such as tight shoals between the group and reduced preference to the live conspecific. Collectively, the data from the novel tank, light/dark, and social behaviour tasks suggest that chronic exposure to Mn elicited both motor abnormalities and anxiety in adult zebrafish. Previously, anxiogenic effects were documented in adult zebrafish chronically exposed to Mn (Zimmermann Prado Rodrigues et al., 2020). These deficits were mechanistically linked to changes in the dopaminergic system, as evidenced by an increased level of DOPAC. The observed anxiogenic behavioural response in

the current study aligns with findings from studies involving zebrafish exposed to other metals, such as **nickel** (Nabinger et al., 2018), arsenic (Baldissarelli et al., 2012), aluminium (Haridevamuthu, Raj, et al., 2023), **zinc** (Sarasamma et al., 2018), and **mercury** (Pereira et al., 2016). These collective results suggest that metal contaminants, even at low concentrations, have the potential to alter fish behaviour, indicating a commonality in the behavioural impact of various metal exposures in zebrafish.

DZ intervention relieves the symptoms and increases exploration as well as time spent in the top region. DZ improves the motor response, as evident by increased swimming distance and speed. DZ improves the risk assessment approach and enhances the exploration of the light region. DZ also relieves the tight shoal and enhances the intrasocial responses by increasing the time in live conspecifics. Oestrogens and androgens are recognized for their significant anxiolytic effects (Zeng et al., 2010). Dietary soy phytoestrogen also has been shown to reduce anxiety in rats and is correlated with this study (Lund & Lephart, 2001). DZ was proven to attenuate depression-like behaviour in rodent models (Chen et al., 2021). DMT1 exhibits high expression in the olfactory epithelium and is essential for Mn transport across this specific tissue, as demonstrated in studies conducted in rats (Thompson et al., 2007). This leaves the olfactory system susceptible to Mn-induced dysfunction. Zebrafish exposed to Mn also exhibited a lesser olfactory preference towards amino acid stimuli, which was corroborated by the Mn attack (Thompson et al., 2007). DZ improves the olfactory function, as evident by increased preference and time for the amino acid region. This improvement is due to the antioxidant effect exerted by DZ, which leads to reduced oxidative damage in olfactory cells. These findings demonstrated that DZ reduces Mn-induced brain injury and improves functional outcomes due to its antioxidant properties.

5 | CONCLUSION

This study demonstrated the beneficial effect of DZ in ameliorating nonmotor symptoms of Mn-induced Parkinsonism. DZ effectively reduced the anxiety-like symptoms and improved social behaviour and olfactory function. Moreover, DZ mitigated oxidative stress, maintained antioxidant status and dopamine levels, and preserved neuronal integrity, collectively contributing to its neuroprotective properties. These findings underscore the therapeutic potential of DZ in addressing heavy metal-induced neurotoxicity, especially Mn-induced Parkinsonism, shedding light on its therapeutic relevance for neurodegenerative disorders. Further investigations are warranted to explore the translation of these outcomes to the clinical application of Mn-induced Parkinsonism.

AUTHOR CONTRIBUTIONS

Balasubramanian Haridevamuthu: Conceptualization (lead); investigation (lead); methodology (lead); writing—original draft (lead). **Gokul Sudhakaran:** Investigation (supporting); writing—original draft (supporting). **Raman Pachiappan:** Data curation (supporting); formal

analysis (supporting); investigation (supporting). **Muthu Kumaradoss Kathiravan:** Formal analysis supporting); investigation (supporting); methodology (supporting). **Krishnan Manikandan:** Formal analysis (supporting); investigation (supporting); methodology (supporting). **Mikhliid H. Almutairi:** Data curation (supporting); formal analysis (supporting); funding acquisition (supporting); investigation (supporting); methodology (supporting); resources (supporting). **Bader O. Almutairi:** Data curation (supporting); formal analysis (supporting); funding acquisition (supporting); methodology (supporting); resources (supporting). **Selvaraj Arokiyaraj:** Data curation (supporting); formal analysis (supporting); funding acquisition (supporting); investigation (supporting); methodology (supporting); resources (supporting). **Jesu Arockiaraj:** Conceptualization (lead); funding acquisition (lead); project administration (lead); resources (lead); supervision (lead); visualization (lead); writing—review and editing (lead).

ACKNOWLEDGEMENTS

The authors express their sincere thanks to the Researchers Supporting Project Number (RSP2024R414), King Saud University, Riyadh, Saudi Arabia.

CONFLICT OF INTEREST STATEMENT

The authors declare that they have no known competing financial interests or personal relationships that could have appeared to influence the work reported in this paper.

DATA AVAILABILITY STATEMENT

The data that support the findings of this study are available from the corresponding author upon reasonable request. Some data may not be made available because of privacy or ethical restrictions.

DECLARATION OF TRANSPARENCY AND SCIENTIFIC RIGOUR

This Declaration acknowledges that this paper adheres to the principles for transparent reporting and scientific rigour of preclinical research as stated in the *BJP* guidelines for **Natural Product Research**, **Design and Analysis**, and **Animal Experimentation**, and as recommended by funding agencies, publishers, and other organizations engaged with supporting research.

ORCID

Balasubramanian Haridevamuthu  <https://orcid.org/0000-0003-4598-5993>
Gokul Sudhakaran  <https://orcid.org/0000-0001-6407-0583>
Raman Pachiappan  <https://orcid.org/0000-0003-2739-4882>
Muthu Kumaradoss Kathiravan  <https://orcid.org/0000-0001-8357-2730>
Krishnan Manikandan  <https://orcid.org/0000-0001-7434-8067>
Mikhliid H. Almutairi  <https://orcid.org/0000-0002-0337-6412>
Bader O. Almutairi  <https://orcid.org/0000-0002-4697-5204>
Selvaraj Arokiyaraj  <https://orcid.org/0000-0002-5486-7246>
Jesu Arockiaraj  <https://orcid.org/0000-0002-0240-7141>

REFERENCES

- Abu-Elfotuh, K., Hamdan, A. M. E., Mohammed, A. A., Atwa, A. M., Kozman, M. R., Ibrahim, A. M., Motawea, S. M., Selim, H. M. R. M., Tohamy, S. T. K., Nour El-Din, M. N., Zaghloul, S. S., Gowifel, A. M. H., & Awny, M. M. (2022). Neuroprotective effects of some nutraceuticals against manganese-induced Parkinson's disease in rats: Possible modulatory effects on TLR4/NLRP3/NF- κ B, GSK-3 β , Nrf2/HO-1, and apoptotic pathways. *Pharmaceuticals*, 15(12), 1554. <https://doi.org/10.3390/ph15121554>
- Alexander, S. P. H., Kelly, E., Mathie, A. A., Peters, J. A., Veale, E. L., Armstrong, J. F., Buneman, O. P., Faccenda, E., Harding, S. D., Spedding, M., Cidrowski, J. A., Fabbro, D., Davenport, A. P., Striessnig, J., Davies, J. A., Ahlers-Dannen, K. E., Alqinyah, M., Arumugam, T. V., Bodle, C., ... Zolghadri, Y. (2023). The Concise Guide to PHARMACOLOGY 2023/24: Introduction and Other Protein Targets. *British Journal of Pharmacology*, 180, S1–S22. <https://doi.org/10.1111/bph.16176>
- Alshehri, M. M., Sharifi-Rad, J., Herrera-Bravo, J., Jara, E. L., Salazar, L. A., Kregiel, D., Upreti, Y., Akram, M., Iqbal, M., Martorell, M., Torrens-Mas, M., Pons, D. G., Daştan, S. D., Cruz-Martins, N., Ozdemir, F. A., Kumar, M., & Cho, W. C. (2021). Therapeutic potential of isoflavones with an emphasis on daidzein. *Oxidative Medicine and Cellular Longevity*, 2021, 6331630. <https://doi.org/10.1155/2021/6331630>
- Altenhofen, S., Wiprich, M. T., Nery, L. R., Leite, C. E., Vianna, M. R. M. R., & Bonan, C. D. (2017). Manganese (II) chloride alters behavioral and neurochemical parameters in larvae and adult zebrafish. *Aquatic Toxicology*, 182, 172–183. <https://doi.org/10.1016/j.aquatox.2016.11.013>
- Anjum, A., Biswas, S., Rahman, M., Rahman, A., Siddique, A. E., Karim, Y., Aktar, S., Nikkon, F., Haque, A., Himeno, S., Hossain, K., & Saud, Z. A. (2019). Butyrylcholinesterase—A potential plasma biomarker in manganese-induced neurobehavioral changes. *Environmental Science and Pollution Research*, 26(7), 6378–6387. <https://doi.org/10.1007/s11356-018-04066-1>
- Ávila, D. S., Rocha, J. B. T., Tizabi, Y., dos Santos, A. P. M., Santamaría, A., Bowman, A. B., & Aschner, M. (2021). Manganese neurotoxicity. In *Handbook of neurotoxicity* (pp. 1–26). Springer International Publishing. https://doi.org/10.1007/978-3-030-71519-9_3-1
- Aziz, N., Kang, Y.-G., Kim, Y.-J., Park, W.-S., Jeong, D., Lee, J., Kim, D., & Cho, J. Y. (2020). Regulation of 8-hydroxydaidzein in IRF3-mediated gene expression in LPS-stimulated murine macrophages. *Biomolecules*, 10(2), 238. <https://doi.org/10.3390/biom10020238>
- Baldissarelli, L. A., Capiotti, K. M., Bogo, M. R., Ghisleni, G., & Bonan, C. D. (2012). Arsenic alters behavioral parameters and brain ectonucleotidases activities in zebrafish (*Danio rerio*). *Comparative Biochemistry and Physiology Part C: Toxicology & Pharmacology*, 155(4), 566–572. <https://doi.org/10.1016/j.cbpc.2012.01.006>
- Boopathi, S., Haridevamuthu, B., Mendonca, E., Gandhi, A., Priya, P. S., Alkahtani, S., al-Johani, N. S., Arokiyaraj, S., Guru, A., Arockiaraj, J., & Malafaia, G. (2023). Combined effects of a high-fat diet and polyethylene microplastic exposure induce impaired lipid metabolism and locomotor behavior in larvae and adult zebrafish. *Science of the Total Environment*, 902, 165988. <https://doi.org/10.1016/j.scitotenv.2023.165988>
- Boopathi, S., Mendonca, E., Gandhi, A., Rady, A., Darwish, N. M., Arokiyaraj, S., Kumar, T. T. A., Pachaiappan, R., Guru, A., & Arockiaraj, J. (2024). Exploring the combined effect of exercise and apigenin on aluminium-induced neurotoxicity in zebrafish. *Molecular Neurobiology*. <https://doi.org/10.1007/s12035-024-03913-2>
- Bradford, M. (1976). A rapid and sensitive method for the quantitation of microgram quantities of protein utilizing the principle of protein-dye binding. *Analytical Biochemistry*, 72(1–2), 248–254. <https://doi.org/10.1006/abio.1976.9999>
- Chen, L., Wang, X., Zhang, Y., Zhong, H., Wang, C., Gao, P., & Li, B. (2021). Daidzein alleviates hypothalamic-pituitary-adrenal axis hyperactivity, ameliorates depression-like behavior, and partly rectifies circulating cytokine imbalance in two rodent models of depression. *Frontiers in Behavioral Neuroscience*, 15, 671864. <https://doi.org/10.3389/fnbeh.2021.671864>
- Claus Henn, B., Ettinger, A. S., Schwartz, J., Téllez-Rojo, M. M., Lamadrid-Figueroa, H., Hernández-Avila, M., Schnaas, L., Amarasiwardena, C., Bellinger, D. C., Hu, H., & Wright, R. O. (2010). Early postnatal blood manganese levels and children's neurodevelopment. *Epidemiology*, 21(4), 433–439. <https://doi.org/10.1097/EDE.0b013e3181df8e52>
- Curtis, M. J., Alexander, S., Cirino, G., Docherty, J. R., George, C. H., Giembycz, M. A., Hoyer, D., Insel, P. A., Izzo, A. A., Ji, Y., MacEwan, D. J., Sobey, C. G., Stanford, S. C., Teixeira, M. M., Wonnacott, S., & Ahluwalia, A. (2018). Experimental design and analysis and their reporting II: Updated and simplified guidance for authors and peer reviewers. *British Journal of Pharmacology*, 175(7), 987–993. <https://doi.org/10.1111/bph.14153>
- Curtis, M. J., Alexander, S. P. H., Cirino, G., George, C. H., Kendall, D. A., Insel, P. A., Izzo, A. A., Ji, Y., Panettieri, R. A., Patel, H. H., Sobey, C. G., Stanford, S. C., Stanley, P., Stefanska, B., Stephens, G. J., Teixeira, M. M., Vergnolle, N., & Ahluwalia, A. (2022). Planning experiments: Updated guidance on experimental design and analysis and their reporting III. *British Journal of Pharmacology*, 179(15), 3907–3913. Portico. <https://doi.org/10.1111/bph.15868>
- de Sá-Nakanishi, A. B., Soares, A. A., de Oliveira, A. L., Fernando Comar, J., Peralta, R. M., & Bracht, A. (2014). Effects of treating old rats with an aqueous *Agaricus blazei* extract on oxidative and functional parameters of the brain tissue and brain mitochondria. *Oxidative Medicine and Cellular Longevity*, 2014, 563179. <https://doi.org/10.1155/2014/563179>
- Dorsey, E. R., Sherer, T., Okun, M. S., & Bloem, B. R. (2018). The emerging evidence of the Parkinson pandemic. *Journal of Parkinson's Disease*, 8(s1), S3–S8. <https://doi.org/10.3233/JPD-181474>
- Doyle, J. M., & Croll, R. P. (2022). A critical review of zebrafish models of Parkinson's disease. *Frontiers in Pharmacology*, 13, 835827. <https://doi.org/10.3389/fphar.2022.835827>
- Ellerby, L. M., & Bredesen, D. E. (2000). Measurement of cellular oxidation, reactive oxygen species, and antioxidant enzymes during apoptosis. *Methods in Enzymology*, 322, 413–421. [https://doi.org/10.1016/S0076-6879\(00\)22040-5](https://doi.org/10.1016/S0076-6879(00)22040-5)
- Ellman, G. L., Courtney, K. D., Andres, V., & Featherstone, R. M. (1961). A new and rapid colorimetric determination of acetylcholinesterase activity. *Biochemical Pharmacology*, 7(2), 88–95. [https://doi.org/10.1016/0006-2952\(61\)90145-9](https://doi.org/10.1016/0006-2952(61)90145-9)
- Erikson, K. M., & Aschner, M. (2003). Manganese neurotoxicity and glutamate-GABA interaction. *Neurochemistry International*, 43(4–5), 475–480. [https://doi.org/10.1016/S0197-0186\(03\)00037-8](https://doi.org/10.1016/S0197-0186(03)00037-8)
- Faria, M., Ziv, T., Gómez-Canela, C., Ben-Lulu, S., Prats, E., Novoa-Luna, K. A., Admon, A., Piña, B., Tauler, R., Gómez-Oliván, L. M., & Raldúa, D. (2018). Acrylamide acute neurotoxicity in adult zebrafish. *Scientific Reports*, 8(1), 7918. <https://doi.org/10.1038/s41598-018-26343-2>
- Feigin, V. L., Abajobir, A. A., Abate, K. H., Abd-Allah, F., Abdulle, A. M., Abera, S. F., Abyu, G. Y., Ahmed, M. B., Aichour, A. N., Aichour, I., Aichour, M. T. E., Akinyemi, R. O., Alabed, S., Al-Raddadi, R., Alvis-Guzman, N., Amare, A. T., Ansari, H., Anwar, P., Ärnlöv, J., ... Vos, T. (2017). Global, regional, and national burden of neurological disorders during 1990–2015: A systematic analysis for the Global Burden of Disease Study 2015. *The Lancet Neurology*, 16(11), 877–897. [https://doi.org/10.1016/S1474-4422\(17\)30299-5](https://doi.org/10.1016/S1474-4422(17)30299-5)
- Ferreira, S. A., Loreto, J. S., dos Santos, M. M., & Barbosa, N. V. (2022). Environmentally relevant manganese concentrations evoke anxiety phenotypes in adult zebrafish. *Environmental Toxicology and Pharmacology*, 93, 103870. <https://doi.org/10.1016/j.etap.2022.103870>
- Ganie, S. A., Haq, E., Hamid, A., Qurishi, Y., Mahmood, Z., Zargar, B. A., Masood, A., & Zargar, M. A. (2011). Carbon tetrachloride induced

- kidney and lung tissue damages and antioxidant activities of the aqueous rhizome extract of *Podophyllum hexandrum*. *BMC Complementary and Alternative Medicine*, 11, 17. <https://doi.org/10.1186/1472-6882-11-17>
- Goel, R., & Chaudhary, R. (2020). Effect of daidzein on Parkinson disease induced by reserpine in rats. *Brazilian Journal of Pharmaceutical Sciences*, 56, e18388. <https://doi.org/10.1590/s2175-97902019000318388>
- Goldman, S. M. (2014). Environmental toxins and Parkinson's disease. *Annual Review of Pharmacology and Toxicology*, 54(1), 141–164. <https://doi.org/10.1146/annurev-pharmtox-011613-135937>
- Gupta, T., & Mullins, M. C. (2010). Dissection of organs from the adult zebrafish. *Journal of Visualized Experiments*, 37, e1717. <https://doi.org/10.3791/1717>
- Guru, A., Sudhakaran, G., Velayutham, M., Murugan, R., Pachaiappan, R., Mothana, R. A., Noman, O. M., Juliet, A., & Arockiaraj, J. (2022). Daidzein normalized gentamicin-induced nephrotoxicity and associated pro-inflammatory cytokines in MDCK and zebrafish: Possible mechanism of nephroprotection. *Comparative Biochemistry and Physiology Part C: Toxicology & Pharmacology*, 258, 109364. <https://doi.org/10.1016/j.cbpc.2022.109364>
- Haridevamuthu, B., Murugan, R., Seenivasan, B., Meenatchi, R., Pachaiappan, R., Almutairi, B. O., Arockiaraj, S., & Arockiaraj, J. (2024). Synthetic azo-dye, Tartrazine induces neurodevelopmental toxicity via mitochondria-mediated apoptosis in zebrafish embryos. *Journal of Hazardous Materials*, 461, 132524. <https://doi.org/10.1016/j.jhazmat.2023.132524>
- Haridevamuthu, B., Raj, D., Kesavan, D., Muthuraman, S., Kumar, R. S., Mahboob, S., Al-Ghanim, K. A., Almutairi, B. O., Arockiaraj, S., Gopinath, P., & Arockiaraj, J. (2023). Trihydroxy piperlongumine protects aluminium induced neurotoxicity in zebrafish: Behavioral and biochemical approach. *Comparative Biochemistry and Physiology Part - C: Toxicology and Pharmacology*, 268, 109600. <https://doi.org/10.1016/j.cbpc.2023.109600>
- Haridevamuthu, B., Seenivasan, B., Priya, P. S., Muthuraman, S., Kumar, R. S., Manikandan, K., Almutairi, B. O., Almutairi, M. H., Arockiaraj, S., Gopinath, P., & Arockiaraj, J. (2023). Hepatoprotective effect of dihydroxy piperlongumine in high cholesterol-induced non-alcoholic fatty liver disease zebrafish via antioxidant activity. *European Journal of Pharmacology*, 945, 175605. <https://doi.org/10.1016/j.ejphar.2023.175605>
- Harischandra, D. S., Ghaisas, S., Zenitsky, G., Jin, H., Kanthasamy, A., Anantharam, V., & Kanthasamy, A. G. (2019). Manganese-induced neurotoxicity: New insights into the triad of protein misfolding, mitochondrial impairment, and neuroinflammation. *Frontiers in Neuroscience*, 13, 654. <https://doi.org/10.3389/fnins.2019.00654>
- Izzo, A. A., Teixeira, M., Alexander, S. P., Cirino, G., Docherty, J. R., George, C. H., Insel, P. A., Ji, Y., Kendall, D. A., Panattieri, R. A., Sobey, C. G., Stanford, S. C., Stefanska, B., Stephens, G., & Ahluwalia, A. (2020). A practical guide for transparent reporting of research on natural products in the British Journal of Pharmacology: Reproducibility of natural product research. *British Journal of Pharmacology*, 177(10), 2169–2178. <https://doi.org/10.1111/bph.15054>
- Jaiswal, S., Goyal, A., & Garabadu, D. (2023). Daidzein attenuates ovariectomy-induced cognitive deficits by improving cortical endothelial function in rats. *Revista Brasileira de Farmacognosia*, 33(5), 1001–1011. <https://doi.org/10.1007/s43450-023-00425-3>
- Kaluff, A. V., Gebhardt, M., Stewart, A. M., Cachat, J. M., Brimmer, M., Chawla, J. S., Craddock, C., Kyzar, E. J., Roth, A., Landsman, S., Gaikwad, S., Robinson, K., Baatrup, E., Tierney, K., Shamchuk, A., Norton, W., Miller, N., Nicolson, T., Braubach, O., ... Zebrafish Neuroscience Research Consortium. (2013). Towards a Comprehensive Catalog of Zebrafish Behavior 1.0 and Beyond. *Zebrafish*, 10(1), 70–86. <https://doi.org/10.1089/zeb.2012.0861>
- Kinkel, M. D., Eames, S. C., Philipson, L. H., & Prince, V. E. (2010). Intraperitoneal injection into adult zebrafish. *Journal of Visualized Experiments*, 42, e2126. <https://doi.org/10.3791/2126>
- Koide, T., Miyasaka, N., Morimoto, K., Asakawa, K., Urasaki, A., Kawakami, K., & Yoshihara, Y. (2009). Olfactory neural circuitry for attraction to amino acids revealed by transposon-mediated gene trap approach in zebrafish. *Proceedings of the National Academy of Sciences*, 106(24), 9884–9889. <https://doi.org/10.1073/pnas.0900470106>
- Kwakye, G., Paoliello, M., Mukhopadhyay, S., Bowman, A., & Aschner, M. (2015). Manganese-induced Parkinsonism and Parkinson's disease: Shared and distinguishable features. *International Journal of Environmental Research and Public Health*, 12(7), 7519–7540. <https://doi.org/10.3390/ijerph120707519>
- Li, Y., He, G., Chen, D., Yu, B., Yu, J., Zheng, P., Huang, Z., Luo, Y., Luo, J., Mao, X., Yan, H., & He, J. (2021). Supplementing daidzein in diets improves the reproductive performance, endocrine hormones and antioxidant capacity of multiparous sows. *Animal Nutrition*, 7(4), 1052–1060. <https://doi.org/10.1016/j.aninu.2021.09.002>
- Lilley, E., Stanford, S. C., Kendall, D. E., Alexander, S. P. H., Cirino, G., Docherty, J. R., George, C. H., Insel, P. A., Izzo, A. A., Ji, Y., Panettieri, R. A., Sobey, C. G., Stefanska, B., Stephens, G., Teixeira, M., & Ahluwalia, A. (2020). ARRIVE 2.0 and the British Journal of Pharmacology: Updated guidance for 2020. *British Journal of Pharmacology*, 177(16), 3611–3616. <https://doi.org/10.1111/bph.15178>
- Lund, T. D., & Lephart, E. D. (2001). Dietary soy phytoestrogens produce anxiolytic effects in the elevated plus-maze. *Brain Research*, 913(2), 180–184. [https://doi.org/10.1016/S0006-8993\(01\)02793-7](https://doi.org/10.1016/S0006-8993(01)02793-7)
- Marklund, S., & Marklund, G. (1974). Involvement of the superoxide anion radical in the autoxidation of pyrogallol and a convenient assay for superoxide dismutase. *European Journal of Biochemistry*, 47(3), 469–474. <https://doi.org/10.1111/j.1432-1033.1974.tb03714.x>
- Maximino, C., Meinerz, D. L., Fontana, B. D., Mezzomo, N. J., Stefanello, F. V., Prestes, A. D. S., Batista, C. B., Rubin, M. A., Barbosa, N. V., Rocha, J. B. T., Lima, M. G., & Rosenberg, D. B. (2018). Extending the analysis of zebrafish behavioral endophenotypes for modeling psychiatric disorders: Fear conditioning to conspecific alarm response. *Behavioural Processes*, 149, 35–42. <https://doi.org/10.1016/j.beproc.2018.01.020>
- Mezzomo, N. J., Silveira, A., Giuliani, G. S., Quadros, V. A., & Rosenberg, D. B. (2016). The role of taurine on anxiety-like behaviors in zebrafish: A comparative study using the novel tank and the light-dark tasks. *Neuroscience Letters*, 613, 19–24. <https://doi.org/10.1016/j.neulet.2015.12.037>
- Miller, N., & Gerlai, R. (2007). Quantification of shoaling behaviour in zebrafish (*Danio rerio*). *Behavioural Brain Research*, 184(2), 157–166. <https://doi.org/10.1016/j.bbr.2007.07.007>
- Nabinger, D. D., Altenhofen, S., Bitencourt, P. E. R., Nery, L. R., Leite, C. E., Vianna, M. R. M. R., & Bonan, C. D. (2018). Nickel exposure alters behavioral parameters in larval and adult zebrafish. *Science of the Total Environment*, 624, 1623–1633. <https://doi.org/10.1016/j.scitotenv.2017.10.057>
- Nadig, A. P. R., Huwaimel, B., Alobaida, A., Khafagy, E.-S., Alotaibi, H. F., Moin, A., Lila, A. S. A., Suman, M., & Krishna, K. L. (2022). Manganese chloride (MnCl₂) induced novel model of Parkinson's disease in adult zebrafish; involvement of oxidative stress, neuroinflammation and apoptosis pathway. *Biomedicine & Pharmacotherapy*, 155, 113697. <https://doi.org/10.1016/j.biopha.2022.113697>
- Nkpaa, K. W., Nkpaa, B. B., Amadi, B. A., Ogbolosingha, A. J., Wopara, I., Belonwu, D. C., Patrick-Iwuanyanwu, K. C., Nwaichi, E. O., Wegwu, M. O., & Orisakwe, O. E. (2022). Selenium abates manganese-induced striatal and hippocampal toxicity via abrogation of neurobehavioral deficits, biometal accumulation, oxidative stress, inflammation, and caspase-3 activation in rats. *Psychopharmacology*, 239(2), 399–412. <https://doi.org/10.1007/s00213-021-06010-7>

- OECD. (2019). Test No. 203: Fish, acute toxicity test. In *OECD guidelines for the testing of chemicals, section 2* (pp. 1–22). OECD Publishing. <https://doi.org/10.1787/9789264069961-en>
- Ohkawa, H., Ohishi, N., & Yagi, K. (1979). Assay for lipid peroxides in animal tissues by thiobarbituric acid reaction. *Analytical Biochemistry*, 95(2), 351–358. [https://doi.org/10.1016/0003-2697\(79\)90738-3](https://doi.org/10.1016/0003-2697(79)90738-3)
- Percie du Sert, N., Hurst, V., Ahluwalia, A., Alam, S., Avey, M. T., Baker, M., Browne, W. J., Clark, A., Cuthill, I. C., Dirnagl, U., Emerson, M., Garner, P., Holgate, S. T., Howells, D. W., Karp, N. A., Lazic, S. E., Lidster, K., MacCallum, C. J., Macleod, M., ... Würbel, H. (2020). The ARRIVE guidelines 2.0: Updated guidelines for reporting animal research. *PLoS Biology*, 18(7), e3000410. <https://doi.org/10.1371/journal.pbio.3000410>
- Pereira, P., Puga, S., Cardoso, V., Pinto-Ribeiro, F., Raimundo, J., Barata, M., Pousão-Ferreira, P., Pacheco, M., & Almeida, A. (2016). Inorganic mercury accumulation in brain following waterborne exposure elicits a deficit on the number of brain cells and impairs swimming behavior in fish (white seabream—*Diplodus sargus*). *Aquatic Toxicology*, 170, 400–412. <https://doi.org/10.1016/j.aquatox.2015.11.031>
- Pham, M., Raymond, J., Hester, J., Kyzar, E., Gaikwad, S., Bruce, I., Fryar, C., Chanin, S., Enriquez, J., Bagawandoss, S., Zapolsky, I., Green, J., Stewart, A. M., Robison, B. D., & Kalueff, A. V. (2012). Assessing Social Behavior Phenotypes in Adult Zebrafish: Shoaling, Social Preference, and Mirror Biting Tests (pp. 231–246). https://doi.org/10.1007/978-1-61779-597-8_17
- Pyatha, S., Kim, H., Lee, D., & Kim, K. (2022). Association between heavy metal exposure and Parkinson's disease: A review of the mechanisms related to oxidative stress. *Antioxidants*, 11(12), 2467. <https://doi.org/10.3390/antiox11122467>
- Racette, B. A., Nelson, G., Dlamini, W. W., Hershey, T., Prathibha, P., Turner, J. R., Checkoway, H., Sheppard, L., & Searles Nielsen, S. (2021). Depression and anxiety in a manganese-exposed community. *Neurotoxicology*, 85, 222–233. <https://doi.org/10.1016/j.neuro.2021.05.017>
- Sarasamma, S., Audira, G., Juniardi, S., Sampurna, B., Liang, S.-T., Hao, E., Lai, Y.-H., & Hsiao, C.-D. (2018). Zinc chloride exposure inhibits brain acetylcholine levels, produces neurotoxic signatures, and diminishes memory and motor activities in adult zebrafish. *International Journal of Molecular Sciences*, 19(10), 3195. <https://doi.org/10.3390/ijms19103195>
- Song, C., Yang, L., Wang, J., Chen, P., Li, S., Liu, Y., Nguyen, M., Kaluyeva, A., Kyzar, E. J., Gaikwad, S., & Kalueff, A. V. (2016). Building neurophenomics in zebrafish: Effects of prior testing stress and test batteries. *Behavioural Brain Research*, 311, 24–30. <https://doi.org/10.1016/j.bbr.2016.05.005>
- Tarale, P., Chakrabarti, T., Sivanesan, S., Naoghare, P., Bafana, A., & Krishnamurthi, K. (2016). Potential role of epigenetic mechanism in manganese induced neurotoxicity. *BioMed Research International*, 2016, 2548792. <https://doi.org/10.1155/2016/2548792>
- Thompson, K., Molina, R. M., Donaghey, T., Schwob, J. E., Brain, J. D., & Wessling-Resnick, M. (2007). Olfactory uptake of manganese requires DMT1 and is enhanced by anemia. *The FASEB Journal*, 21(1), 223–230. <https://doi.org/10.1096/fj.06-6710com>
- Tinkov, A. A., Paoliello, M. M. B., Mazilina, A. N., Skalny, A. V., Martins, A. C., Voskresenskaya, O. N., Aaseth, J., Santamaria, A., Notova, S. V., Tsatsakis, A., Lee, E., Bowman, A. B., & Aschner, M. (2021). Molecular targets of manganese-induced neurotoxicity: A five-year update. *International Journal of Molecular Sciences*, 22(9), 4646. <https://doi.org/10.3390/ijms22094646>
- Wang, X., Yin, Z., Meng, X., Yang, D., Meng, H., Liao, C., Wei, L., Chen, Y., Yang, X., Han, J., Duan, Y., & Zhang, S. (2022). Daidzein alleviates neuronal damage and oxidative stress via GSK3 β /Nrf2 pathway in mice. *Journal of Functional Foods*, 92, 105060. <https://doi.org/10.1016/j.jff.2022.105060>
- Wang, Y., Gao, X., Li, X., Ding, Y., Shi, Q., Yang, Z., Peng, D., & Liu, H. (2023). Design, synthesis and the evaluation of cholinesterase inhibition and blood-brain permeability of daidzein derivatives or analogs. *Chemical Biology & Drug Design*, 102(4), 718–729. <https://doi.org/10.1111/cbdd.14279>
- Wu, Q., Wang, M., Chen, W., Wang, K., & Wang, Y. (2022). Daidzein exerts neuroprotective activity against MPTP-induced Parkinson's disease in experimental mice and lipopolysaccharide-induced BV2 microglial cells. *Journal of Biochemical and Molecular Toxicology*, 36(2), e22949. <https://doi.org/10.1002/jbt.22949>
- Wullimann, M. F., Rupp, B., & Reichert, H. (1996). Neuroanatomy of the zebrafish brain. In *Neuroanatomy of the zebrafish Brain*. Birkhäuser Basel. <https://doi.org/10.1007/978-3-0348-8979-7>
- Yamanaka, O., & Takeuchi, R. (2018). UMATracker: An intuitive image-based tracking platform. *Journal of Experimental Biology*, 221(16), jeb182469. <https://doi.org/10.1242/jeb.182469>
- Yao, Z., Bai, Q., & Wang, G. (2021). Mechanisms of oxidative stress and therapeutic targets following intracerebral hemorrhage. *Oxidative Medicine and Cellular Longevity*, 2021, 8815441. <https://doi.org/10.1155/2021/8815441>
- Zeng, S., Tai, F., Zhai, P., Yuan, A., Jia, R., & Zhang, X. (2010). Effect of daidzein on anxiety, social behavior and spatial learning in male Balb/cJ mice. *Pharmacology Biochemistry and Behavior*, 96(1), 16–23. <https://doi.org/10.1016/j.pbb.2010.03.015>
- Zimmermann Prado Rodrigues, G., Staudt, L. B. M., Moreira, M. G., dos Santos, T. G., de Souza, M. S., Lúcio, C. J., Panizzon, J., Kayser, J. M., Simões, L. A. R., Ziulkoski, A. L., Bonan, C. D., de Oliveira, D. L., & Gehlen, G. (2020). Histopathological, genotoxic, and behavioral damages induced by manganese (II) in adult zebrafish. *Chemosphere*, 244, 125550. <https://doi.org/10.1016/j.chemosphere.2019.125550>

How to cite this article: Haridevamuthu, B., Sudhakaran, G., Pachaiappan, R., Kathiravan, M. K., Manikandan, K., Almutairi, M. H., Almutairi, B. O., Arokiyaraj, S., & Arockiaraj, J. (2024). Daidzein ameliorates nonmotor symptoms of manganese-induced Parkinsonism in zebrafish model: Behavioural and biochemical approach. *British Journal of Pharmacology*, 1–17. <https://doi.org/10.1111/bph.16382>



Neuroprotective potential of pyrazole benzenesulfonamide derivative T1 in targeted intervention against PTZ-induced epilepsy-like condition in *in vivo* zebrafish model

Raghul Murugan^a, S.P. Ramya Ranjan Nayak^a, B. Haridevamuthu^a, D. Priya^b,
Vellapandian Chitra^c, Bader O. Almutairi^d, Selvaraj Arokiyaraj^e, Muthupandian Saravanan^f, M.
K. Kathiravan^{b,*}, Jesu Arockiaraj^{a,*}

^a Toxicology and Pharmacology Laboratory, Department of Biotechnology, Faculty of Science and Humanities, SRM Institute of Science and Technology, Kattankulathur 603203, Chengalpattu District, Tamil Nadu, India

^b Dr APJ Abdul Kalam Research Lab, Department of Pharmaceutical Chemistry, SRM College of Pharmacy, SRM Institute of Science and Technology, Kattankulathur 603203, Chengalpattu District, Tamil Nadu, India

^c Department of Pharmacology, SRM College of Pharmacy, SRM Institute of Science and Technology, Kattankulathur 603203, Chengalpattu District, Tamil Nadu, India

^d Department of Zoology, College of Science, King Saud University, P.O. Box 2455, Riyadh 11451, Saudi Arabia

^e Department of Food Science & Biotechnology, Sejong University, Seoul 05006, Republic of Korea

^f AMR and Nanotherapeutics Laboratory, Department of Pharmacology, Saveetha Dental College, Saveetha Institute of Medical and Technical Sciences (SIMATS), Chennai, Tamil Nadu 600077, India

ARTICLE INFO

Keyword:

Epilepsy

Pyrazole

Neuroprotection

Neuroinflammation

COX-2 inhibitor

ABSTRACT

Epilepsy is a chronic neurological disease characterized by a persistent susceptibility to seizures. Pharmacoresistant epilepsies, impacting around 30 % of patients, highlight the urgent need for improved treatments. Neuroinflammation, prevalent in epileptogenic brain regions, is a key player in epilepsy, prompting the search for new mechanistic therapies. Hence, in this study, we explored the anti-inflammatory potential of pyrazole benzenesulfonamide derivative (T1) against pentylenetetrazole (PTZ) induced epilepsy-like conditions in *in-vivo* zebrafish model. The results from the survival assay showed 79.97 ± 6.65 % at 150 μ M of T1 compared to PTZ-group. The results from reactive oxygen species (ROS), apoptosis and histology analysis showed that T1 significantly reduces cellular damage due to oxidative stress in PTZ-exposed zebrafish. The gene expression analysis and neutral red assay results demonstrated a notable reduction in the inflammatory response in zebrafish pre-treated with T1. Subsequently, the open field test unveiled the anti-convulsant activity of T1, particularly at a concentration of 150 μ M. Moreover, both RT-PCR and immunohistochemistry findings indicated a concentration-dependent potential of T1, which inhibited COX-2 in zebrafish exposed to PTZ. In summary, T1 protected zebrafish against PTZ-induced neuronal damage, and behavioural changes by mitigating the inflammatory response through the inhibition of COX-2.

1. Introduction

Epilepsy is a persistent neurological condition affecting more than 50 million people globally [1]. Epilepsy is marked by recurrent seizures, stemming from a range of physiological, cognitive, and neurobiological disruptions [2]. The most common factors that trigger seizures are cerebrovascular disease, drug withdrawal, traumatic brain injury, fever, infection, and metabolic disorders. Besides, patients with epilepsy experience prolonged seizures and, consequently, are at increased risk of

sudden unexpected death from epilepsy (SUDEP). Current approaches to treating epilepsy encompass the use of anti-epileptic and anti-seizure medications, surgical removal of seizure-triggering brain regions, the implementation of a ketogenic diet, and the implantation of electrical devices for seizure control [3–5]. Although all of these approaches can reduce the frequency of seizures, they cannot cure epilepsy or repair the damage to the neuronal network. Therefore, there is still a need for the development of more effective anti-epileptic drugs. In the current study, we used a pentylenetetrazole (PTZ) induced kindling model to develop

* Corresponding authors.

E-mail addresses: kathirak@srmist.edu.in (M.K. Kathiravan), jesuaroa@srmist.edu.in (J. Arockiaraj).

<https://doi.org/10.1016/j.intimp.2024.111859>

Received 22 December 2023; Received in revised form 10 March 2024; Accepted 11 March 2024

1567-5769/© 2024 Elsevier B.V. All rights reserved.

epileptic conditions in larval and adult zebrafish models. PTZ primarily binds to γ -aminobutyric acid A receptor (GABA_A). The role of GABA in the brain works as an inhibitor for neurotransmittance which is necessary to limit the excitation signals in neural networks [6]. Hence, PTZ exposure causes heightened excitation signals in neural network which results in seizures.

In recent decades, researchers have been investigating the use of anti-inflammatory drugs to prevent epileptogenesis [7]. The neuro-inflammation caused by various stressors contributes to neuronal damage, which was recently explored as a key factor in epileptogenesis. This was corroborated by the increased level of inflammatory cytokines such as $\text{TNF-}\alpha$ and $\text{IL-1}\beta$ in the brains of epileptic patients [8]. Furthermore, seizures associated with epilepsy exacerbate neuroinflammation through signalling pathways involving COX-2 , $\text{TGF-}\beta$, and Toll-like receptors [9]. $\text{TNF-}\alpha$ and $\text{IL-1}\beta$ are secreted by astrocytes and microglia, as an initial event of inflammatory response, which further triggers the production of COX-2 [10]. COX-2 in turn initialise the complement system in neurons, astrocytes and microglia [11]. Hence, targeting the COX-2 enzyme can open doors for the development of potential anti-convulsant drugs for patients with epilepsy. Traditional Indian medical practices extensively utilize plant-derived substances to treat various ailments. *Glycyrrhiza glabra* L. (Licorice) is a notable example of such a medicinal plant, renowned for its effectiveness in managing diverse diseases, including epilepsy. Additionally, Licorice yields numerous chemical compounds with diverse therapeutic potentials [12]. Notably, pyrazole stands out, exhibiting anti-inflammatory properties due to its ability to inhibit COX-2 [13]. Moreover, the versatile five-membered heterocyclic structure of pyrazole makes it suitable for synthesizing various pharmaceutical compounds [14]. In this study, we synthesized a benzenesulfonate-derived analogue (T1) from pyrazole and examined its effects in a zebrafish model under PTZ-induced epilepsy-like conditions.

2. Materials and methods

2.1. Chemicals

Pyrazole benzenesulfonate-derived analogue (T1) (IUPAC: 4-(5-(4-methoxyphenyl)-3-(2-(3-phenoxybenzylidene) hydrazine-1-carbonyl)-1H-pyrazol-1-yl) benzenesulfonamide) was synthesized in the laboratory. PTZ, neutral red, acridine orange, DCFDA (dichlorofluorescein diacetate), sudan black and all the other chemicals used in this study were brought from Sigma Aldrich (MO, USA) or HiMedia Laboratories (Mumbai, India) unless stated.

2.2. Synthesis and characterisation of T1

The synthesis begins with the addition of sodium methoxide to methanol, followed by the incorporation of diethyl oxalate at 0°C . Subsequently, 4-Methoxy acetophenone is dripped into the solution at an ice-cold temperature, followed by refluxing at 60°C . TLC is employed to monitor the reaction's progress. Afterward, the solution is left overnight, and the solvent is removed, adjusting the pH with HCl. The resulting precipitate is washed and subjected to recrystallization. This ester is then reacted with 4-Hydrazinyl benzene sulphonamide in methanol at reflux temperature. The obtained precipitates are filtered, washed, and recrystallized using ethyl acetate. The resulting intermediate is then mixed with hydrazine hydrate and stirred at 80°C . TLC is again used for monitoring. Upon completion, a brine solution is added to obtain the product, which is filtered, washed, and recrystallized. Finally, Pyrazole hydrazide is dissolved in methanol, mixed with 3-phenoxy benzaldehyde and acetic acid, and stirred. The resulting precipitate is filtered, washed, and subjected to recrystallization using ethanol. Throughout the process, TLC is utilized to monitor the reactions' progress, and appropriate washing and recrystallization procedures are employed for purification [15].

P-methoxy acetophenone was reacted with diethyl oxalate in

presence of methanol to yield esters via claisen condensation reaction. The formed enolate ion attacks the esters which undergoes Nu-acyl substitution. The ester obtained was solid with 90 % yield, with melting point $383\text{--}385^\circ\text{C}$. IR for the ester compound showed stretching for C-O ester at 1138 cm^{-1} thus confirming the formation of esters. C = C stretching at 751 cm^{-1} indicates the presence of alkene, C = O stretching at 1680 cm^{-1} confirmed the presence of carbonyl group, C-OH stretching at 3122 cm^{-1} confirmed the presence of alcoholic group. The obtained ester was then reacted with 4-hydrazinyl benzene sulphonamide which undergoes cyclization resulting in the formation of pyrazole ester. The pyrazole ester was solid with 87 % yield and melting point ranging between 195 and 197°C . The pyrazole esters showed S = O stretching at 1325 cm^{-1} confirming the presence of sulphonamide, C = O stretching for esters at 1645 cm^{-1} , C-N stretching at 1149 cm^{-1} and NH stretching in the range of 3097 cm^{-1} confirms the formation of pyrazole and mass spectral analysis confirmed the formation of the product. The esters were then converted to the corresponding hydrazides on treatment with hydrazine hydrate which resulted in the formation of product with 75 % yield. The pyrazole hydrazide obtained was solid with melting point ranging between 192 and 194°C and the formation of hydrazide were confirmed by the presence of C = O stretching at 1690 and NH stretching at $3500\text{--}3400\text{ cm}^{-1}$. Later the hydrazides on condensation with 3-phenoxy benzaldehydes resulted in the targeted compound T1. Compound T1 is a colourless solid, characterised by IR, which revealed the presence of aromatic N-H bond, aldehyde and aromatic ester and sulphonamide. The formation of the compound was confirmed by mass spectra which showed a peak at 568.22 . Further, ^1H NMR, and ^{13}C NMR were used for the confirmation of the synthesized compound, which revealed a singlet peak for amide, methoxy, and imine, doublet peak for aromatic and multiplet for aromatic sulphonamide group.

2.3. Zebrafish maintenance

The four-month-old wild-type zebrafish (*Danio rerio*) were procured from Tarun fish farms (Chennai, India). All the zebrafish were acclimatized to lab conditions ($27 \pm 1^\circ\text{C}$, 14/10 light and dark) before the experiment as previously described [16]. Embryos were obtained by natural spawning as described before [17]. All the animal experiments were performed as per the guidelines of the Committee for Control and Supervision of Experiments on Animals (CCSEA) and approved by the Institutional Animal Care and Use Committee of SRMIST (No. IAEC/312/2023).

2.4. Larvae experimental setup

The embryos at 4 days post-fertilization were carefully examined and healthy ones were split into five different groups as mentioned in Table 1. The concentration of T1 used for the experiments were determined based on the survival assay using developing zebrafish embryo (Fig. S2). After the exposure, zebrafish embryos were immediately processed for further analysis.

Table 1
Grouping of zebrafish larvae for the induction of epilepsy.

Group name	Group detail	Administration details
CONTROL	Healthy	Maintained in E3 medium
PTZ	Model	2 h of PTZ (6 mM)
PTZ + T1 (50 μM)	Pyrazole benzenesulfonate analogue treatment	24 h pre-treatment of T1 (50 μM) followed by 2 h of PTZ (6 mM)
PTZ + T1 (100 μM)		24 h pre-treatment of T1 (100 μM) followed by 2 h of PTZ (6 mM)
PTZ + T1 (150 μM)		24 h pre-treatment of T1 (150 μM) followed by 2 h of PTZ (6 mM)

2.5. Heartbeat and survival rate of zebrafish embryo

PTZ and T1-exposed zebrafish embryos from each experimental group were observed under the Cosmo light microscope (Cosmo Laboratory Equipment, India) and photographed using ScopeImage (Ver. 9.0). The heartbeat of each embryo were counted manually through the microscope and the values were plotted in the graph. Similarly, the number of embryos that survived was plotted in the graph.

2.6. Estimation of reactive oxygen species (ROS) and apoptosis

The ROS and apoptosis in zebrafish larvae were determined as described previously [18]. The zebrafish embryo after treatment were stained with 20 µg/mL of DCFDA dye for 20 min in dark to stain intracellular ROS. Similarly, apoptosis was determined by staining DNA using 20 µg/mL acridine orange dye for 20 min in dark. The zebrafish larvae after staining were washed twice with 1 × PBS and anesthetized by giving hypothermic shock. Anesthetized larvae were then mounted on glass slide and observed under EXC-500 fluorescent microscope (Accu-Scope, NY, USA) and images were captured using CaptaVision + software (Ver. 2.4.1). The intensity of fluorescence was quantified using ImageJ software (NIH, USA).

2.7. Macrophage localization assay

The percentage of macrophages localised at the inflammatory site was stained using neutral red dye as described earlier [19]. Briefly, the zebrafish larvae at the end of the exposure period were stained with 10 µg/mL of neutral red for 30 min. After incubation, the excess stain was washed with 1 × PBS and the larvae were anaesthetized by hypothermic shock. Then the anesthetized larvae were observed under Cosmo light microscope. The percentage of localized macrophages were measured using ImageJ software.

2.8. qPCR analysis

The total RNA was isolated from the supernatant of zebrafish larvae from each group using TRIzol reagent according to manufacturer's protocol. The RNA isolated was quantified using a Nanodrop 2000c spectrophotometer (ThermoFisher Scientific, USA). By using zebrafish specific primers for neural development and inflammatory marker genes and KAPA SYBR FAST one-step qRT-PCR mix kit (KAPA biosystems), the qPCR was performed for genes such as *bdnf* (brain derived neurotrophic factor), *cox-2* (cyclooxygenase-2), *tnf-α* (tumour necrosis factor- alpha) and *il-1β* (interleukin-1 beta) in Light Cycler 96 (Roche, Germany) with *β-actin* as the internal control gene. The information on primers used in the study are listed in Table 2.

2.9. Adult experimental setup

A total of 90 adult zebrafish of both sexes with 18 fish in each group

Table 2
Sequence of primers used in this study. *β- actin* was used as internal reference.

Gene name	Primer	Reference
<i>β- actin</i>	F: CGAGCAGGAGATGGGAACCR: CAACGGAAACGCTCATTTGC	[16]
<i>bdnf</i>	F: CGCGGTACTCTTTCTCTTGGR: CCATTAGTCACGGGGACCTTC	[16]
<i>cox-2</i>	F: AAATGGAAGGCAGCGCCGAGR: TCGGCAGGCTCATCCTTATTGGTGAGACTA	[20]
<i>tnf-α</i>	F: AGGAACAAGTGCTTATGAGCCATGCR: AAATGGAAGGCAGCGCCGAG	[16]
<i>il-1β</i>	F: TCGCCAGTGCTCCGGCTACR: GCAGCTGGTCGTATCCGTTTGG	[16]

with tank duplicate (n = 9) were separated into five experimental groups in a randomized manner as mentioned in Table 3. Drug administration was made via intraperitoneal (i.p.) route strictly adhered to standard procedure as described previously [21]. A vehicle (0.9 % sterile saline solution) was injected to control fish whenever experimental fish were injected with T1. T1 dosages of 50, 10, 150 µM were also chosen based on the maximum tolerated dose in the pilot acute toxicity study (please see Supplementary File). Fish were euthanized by an overdose of buffered tricaine (500 mg/L) and brains were carefully isolated and immediately fixed or processed for further analysis.

2.10. Hematoxylin and eosin staining

The isolated brains (n = 3/ group) from each experimental group were fixed with 10 % formaldehyde for 24 h. The fixed tissue were embedded in paraffin wax and sectioned. Each sections were dewaxed and rehydrated, followed by staining with Hematoxylin and Eosin (H&E) dyes. After staining, the slides were observed under an Accu-Scope brightfield microscope. The morphological changes observed in the brain sections of PTZ and DEA-exposed zebrafish were examined and compared with the control.

2.11. Localization of COX-2 in zebrafish brain

The expression of COX-2 in the brain was determined by immuno-histochemistry (IHC) using a Master polymer plus detection system (Master Diagnostica, Granada). The dewaxed and rehydrated samples were subjected to peroxidase blocking and primary antibody treatments by following the manufacturer's protocol. Then the immunostaining was performed using DAB chromogen. The excess stains were washed with distilled water thrice and samples were covered with haematoxylin for 1–2 min for counterstain. Finally, the samples were washed, dehydrated and mounted for observation under the microscope [22]. The expression of COX-2 was measured using ImageJ software.

2.12. Behavioural analysis

The changes in the behaviour of adult zebrafish from each experimental group was investigated using an open field test as described earlier by Nayak et al. [23] Briefly, the zebrafish from each group were allowed to swim in the open field tank. The behaviour of zebrafish larvae in the tank was recorded using a video camera and tracked using UMATracker software as explained previously [16]. Then the XY-coordinates obtained from the tracking software were plotted using Origin 2019b software. The total distance travelled by each zebrafish was calculated and plotted in graph using Graphpad Prism ver.10 software.

Table 3
Grouping of adult zebrafish for the induction of epilepsy.

Group name	Group detail	Administration details
CONTROL PTZ	Healthy Model	0.9 % sterile saline solution (i.p.) 0.9 % sterile saline solution (i.p.) + 5 min water exposure of PTZ (10 mM) per day with 5 days a week for 4 week.
PTZ + T1 (50 µM)	Pyrazole benzenesulfonate analogue Treatment	T1 (50 µM) (i.p.) + 5 min water exposure of PTZ (10 mM) per day with 5 days a week for 4 week.
PTZ + T1 (100 µM)		T1 (100 µM) (i.p.) + 5 min water exposure of PTZ (10 mM) per day with 5 days a week for 4 week.
PTZ + T1 (150 µM)		T1 (150 µM) (i.p.) + 5 min water exposure of PTZ (10 mM) per day with 5 days a week for 4 week.

2.13. Estimation of GABA in adult zebrafish

The GABA level in adult zebrafish brain was performed using high performance liquid chromatography (HPLC) (Shimadzu, Japan) with SPD-M40 PDA detector as previously explained, with slight modifications [24,25]. Briefly, the adult zebrafish brain ($n = 3/\text{group}$) from each experimental group were homogenized in 0.4 M perchloric acid by sonic homogenizer (Power 55 %, pulse 5 s and stop for 5 s) for 45 s. The resulting supernatant was collected by centrifuging at 13000 rpm for 35 min at 4 °C. Then, the supernatant was filtered using 0.22 μm membrane filter and stored at -80°C until taken for HPLC analysis. The mobile phase used was 16 % of acetonitrile: water (1:1) and 84 % of 0.02 M phosphate buffer (pH 7.0). Ten microliters of each sample were injected into the C18 column ($4.6 \times 250 \text{ mm}$, 5 μm) with the flow rate of 0.450 mL/min. The UV-spectrophotometer detector was set with a wavelength at 230 nm.

2.14. Statistical analysis

Data were presented as mean \pm SD of biological replicates. All the experiments were performed in triplicates and the values obtained were plotted in graph using GraphPad Prism 9.0 software. The normality was tested by the Shapiro–Wilk test and the statistical analysis were performed using ordinary one and two-way analysis of variance (ANOVA) followed by the Dunnett/Bonferroni multiple comparisons test. The $p < 0.05$ was considered a statistically significant difference between groups.

3. Results

3.1. T1 increases survival of PTZ-induced zebrafish larvae

The results of the survival assay (Fig. 1) revealed that the survival rate of zebrafish larvae in the PTZ group was $45.53 \pm 5.08 \%$. Conversely, pre-treatment with T1 led to elevated survival percentages, recording values of $58.87 \pm 5.09 \%$, $72.2 \pm 3.81 \%$, and $79.97 \pm 6.65 \%$ at concentrations of 50, 100, and 150 μM , respectively. Additionally, the results from heartbeat analysis revealed that the PTZ exposure has significantly reduced the heartbeat in zebrafish larvae (83 ± 7) compared to control group. Whereas in T1 treated groups the heartbeat rate was significantly higher to 103 ± 6 ($p < 0.05$), 123 ± 11 ($p < 0.001$) and 157 ± 3 ($p < 0.0001$) at 50, 100 and 150 μM concentrations,

respectively.

3.2. T1 decreases ROS level in PTZ-induced zebrafish larvae

Results from DCFH-DA (Fig. 2) staining analysis indicated a significant increase in fluorescent intensity in zebrafish larvae exposed to PTZ. In contrast, zebrafish larvae pre-treated with T1 displayed a notable reduction in the percentage of fluorescent intensity, measuring $85.01 \pm 2.89 \%$, $54.05 \pm 2.77 \%$, and $35.22 \pm 2.94 \%$ at concentrations of 50, 100, and 150 μM , respectively.

3.3. T1 prevents apoptosis in PTZ-induced zebrafish larvae

The images obtained from the AO staining assay (Fig. 3) demonstrated an increased fluorescent intensity in zebrafish larvae subjected to PTZ. In contrast, T1 pre-treated groups exhibited significantly reduced levels of fluorescent intensity. Specifically, at concentrations of 50, 100, and 150 μM , T1 pre-treatment resulted in a substantial decrease in the percentage of fluorescent intensity to 87.33 ± 2.21 , 73.27 ± 1.09 , and 44.47 ± 2.61 , respectively.

3.4. T1 decreases macrophage localization in PTZ-induced zebrafish larvae

The images obtained from neutral red staining (Fig. 4) revealed a notable increase in localized macrophages in the head region of larvae exposed to PTZ compared to the control group. Additionally, ImageJ analysis results demonstrated a dose-dependent reduction in the percentage of macrophages localized in T1 pre-treated larvae, measuring 73.01 ± 9.16 ($p < 0.05$), 53.18 ± 10.54 ($p < 0.001$), and 30.72 ± 6.02 ($p < 0.0001$) at concentrations of 50, 100, and 150 μM , respectively.

3.5. T1 mitigates the level of inflammatory marker genes

The results from the gene expression analysis were plotted as relative folds of gene expression (Fig. 5). The results revealed that the level of *bdnf* decrease significantly in PTZ group compared with the control group. On contrary, the level of *cox-2*, *tnf- α* and *il-1 β* increased significantly compared to the control group. Whereas, the results from the T1 pre-treated groups revealed that the expression of *bdnf* increased significantly from 0.34 to 0.907 folds ($p < 0.01$) at 150 μM . Additionally, the *cox-2* expression in the PTZ group was decreased from 4.092 folds to

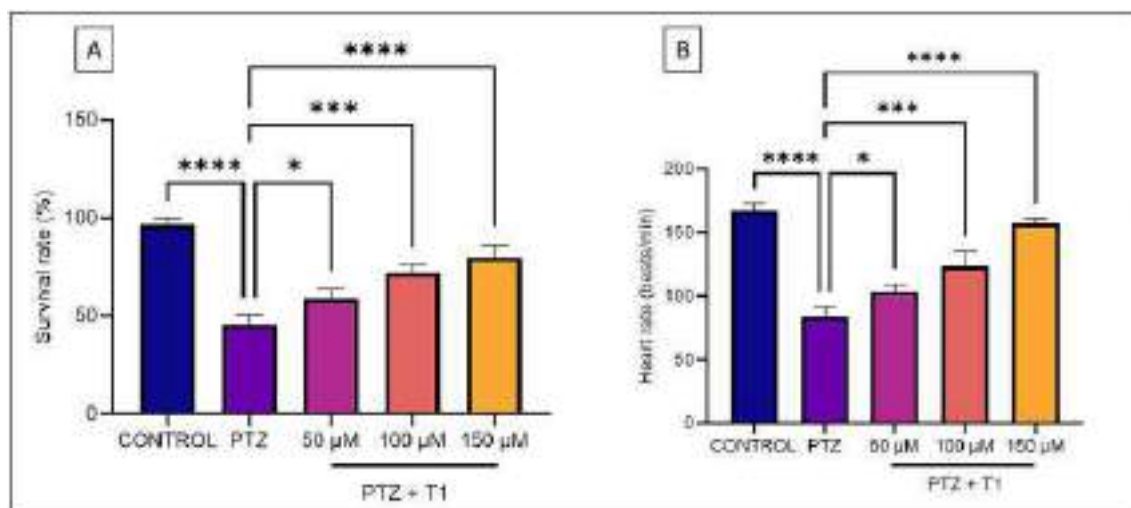


Fig. 1. Representative image for A) Survival rate and B) heart beat rate among the zebrafish larvae from Control, PTZ (6 mM) and T1 at different concentrations (50, 100 and 150 μM) groups. The graph represents the data obtained from triplicates of experiments presented as mean \pm standard deviation. The statistical analysis involved one-way ANOVA followed by Dunnett's multiple comparison test. "*" represents significant difference $p < 0.05$, "****" represents $p < 0.0001$.

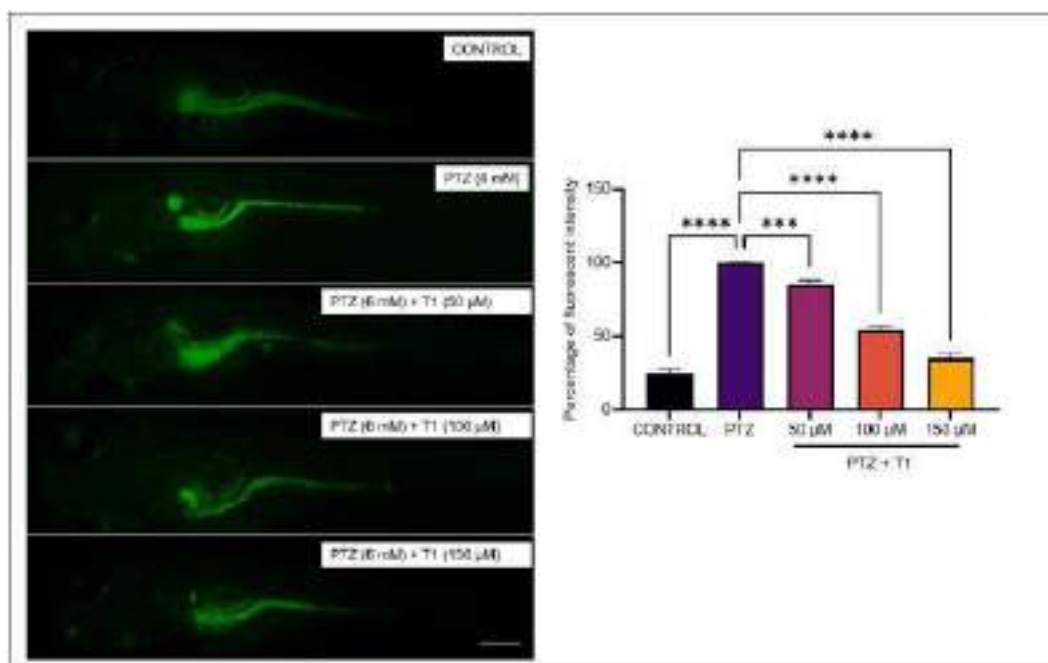


Fig. 2. Representative image for ROS staining using DCFH-DA among the zebrafish larvae from Control, PTZ (6 mM) and T1 at different concentrations (50, 100 and 150 μ M) groups. The graph represents the percentage of fluorescent intensity calculated using ImageJ software. The data were obtained from triplicates of experiments and presented as mean \pm standard deviation. The statistical analysis involved one-way ANOVA followed by Dunnett's multiple comparison test. **** represents $p < 0.0001$ and *** represents $p < 0.001$. Scale- 200 μ m.

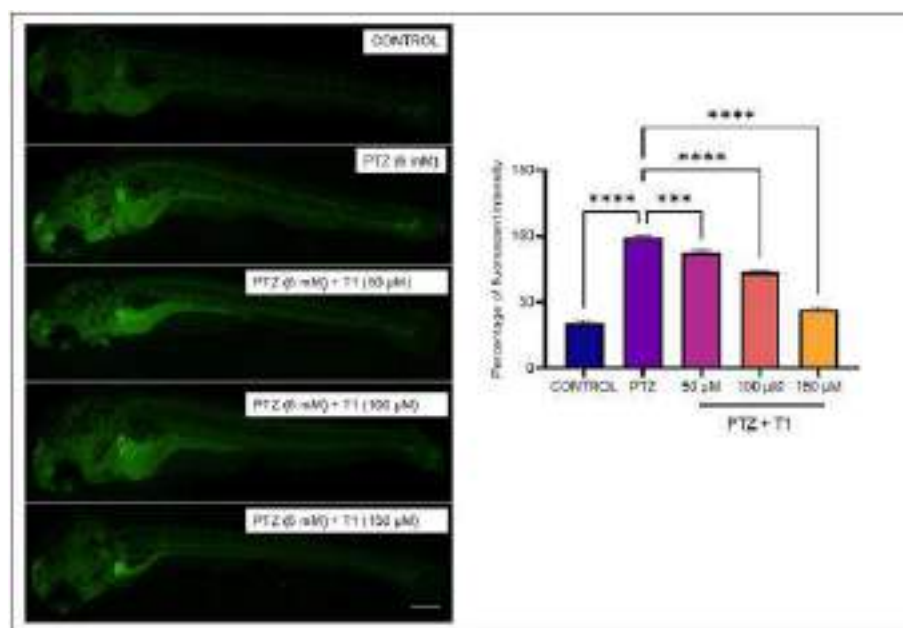


Fig. 3. Illustrates representative images for cellular apoptosis stained using acridine orange for in zebrafish larvae from Control, PTZ (6 mM), and T1 at various concentrations (50, 100, and 150 μ M) groups. The graph depicts the percentage of fluorescent intensity calculated using ImageJ software. Data, derived from triplicate experiments, are presented as mean \pm standard deviation. Statistical analysis involved one-way ANOVA followed by Dunnett's multiple comparison test. **** signifies $p < 0.0001$, and *** signifies $p < 0.001$. Scale- 200 μ m.

3.60, 2.34 ($p < 0.05$) and 1.85 ($p < 0.01$) folds at 50, 100 and 150 μ M concentrations of T1, respectively. Similarly, the expression of *tnf- α* was decreased from 3.79 folds (PTZ group) to 3.34, 2.56 ($p < 0.05$) and 1.55 ($p < 0.05$) folds at 50, 100 and 150 μ M concentrations of T1, respectively. Furthermore, the relative fold of *il-1 β* decreased from 4.40 folds (PTZ group) to 3.55, 3.38 and 1.34 folds at 50, 100 and 150 μ M concentrations of T1, respectively.

3.6. T1 prevents PTZ-induced damage in zebrafish brain

The results from the histology analysis (Fig. 6) revealed that the PTZ-induced kindling caused morphological abnormalities such as pyknosis, haemorrhage, edema, elongated nucleus and degeneration of neurons in the zebrafish brain tissue. Whereas, the brain morphology of T1 treated zebrafish showed a dose-dependent reduction in the tissue abnormalities

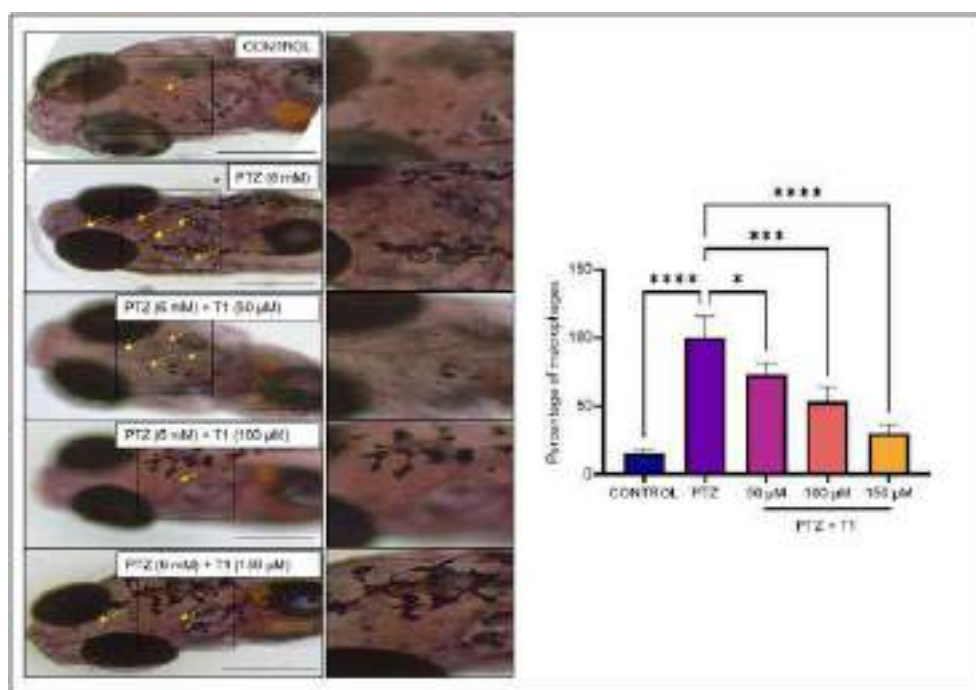


Fig. 4. Illustrates representative images for macrophage localisation stained using neutral red dye in zebrafish larvae from Control, PTZ (6 mM), and T1 at various concentrations (50, 100, and 150 μ M) groups. The graph depicts the percentage of fluorescent intensity calculated using ImageJ software. Data, derived from triplicate experiments, are presented as mean \pm standard deviation. Statistical analysis involved one-way ANOVA followed by Dunnett's multiple comparison test. **** signifies $p < 0.001$, and **** signifies $p < 0.0001$. Scale- 200 μ m.

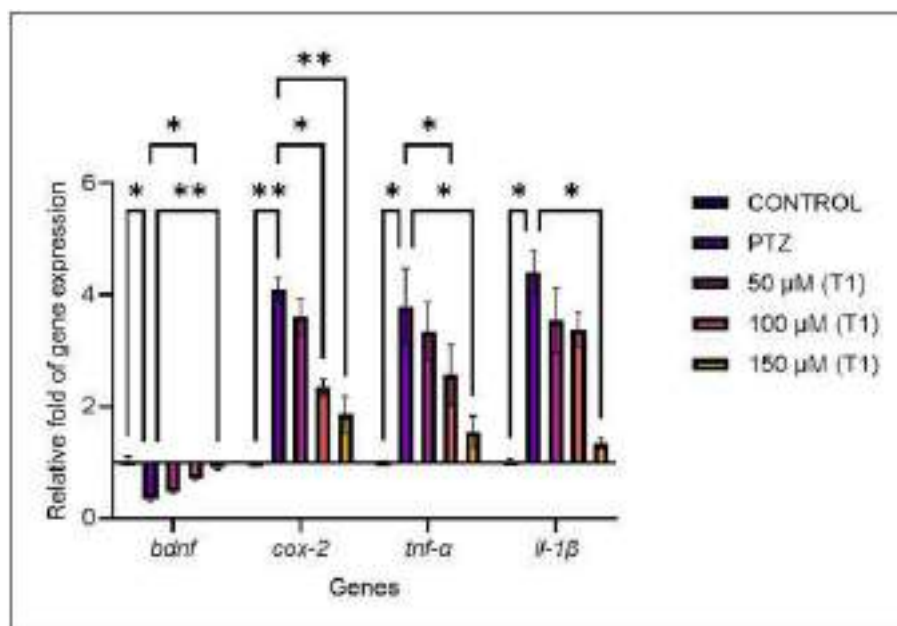


Fig. 5. Representative graph of gene expression analysis for the expression of *bdnf*, *cox-2*, *tnfr-a* and *il-1β* in zebrafish larvae from Control, PTZ (6 mM), and T1 at various concentrations (50, 100, and 150 μ M) groups. The graph depicts the percentage of fluorescent intensity calculated using ImageJ software. Data, derived from triplicate experiments, are presented as mean \pm standard deviation. Statistical analysis involved one-way ANOVA followed by Dunnett's multiple comparison test. * signifies $p < 0.05$ and ** signifies $p < 0.01$.

and at 150 μ M degeneration of neurons was inhibited.

3.7. T1 reduces the expression of COX-2 in brain tissue

The results from the immunohistochemical staining (Fig. 7) demonstrated that the expression of COX-2 enzyme in brain tissue of

PTZ-exposed adult zebrafish was significantly higher compared with the control group. Whereas in T1 treatment groups, the expression of COX-2 decreased significantly to 91.34 ± 1.48 ($p < 0.01$), 77.56 ± 3.29 ($p < 0.0001$) and 64.94 ± 2.01 % ($p < 0.0001$) at 50, 100 and 150 μ M concentrations respectively.

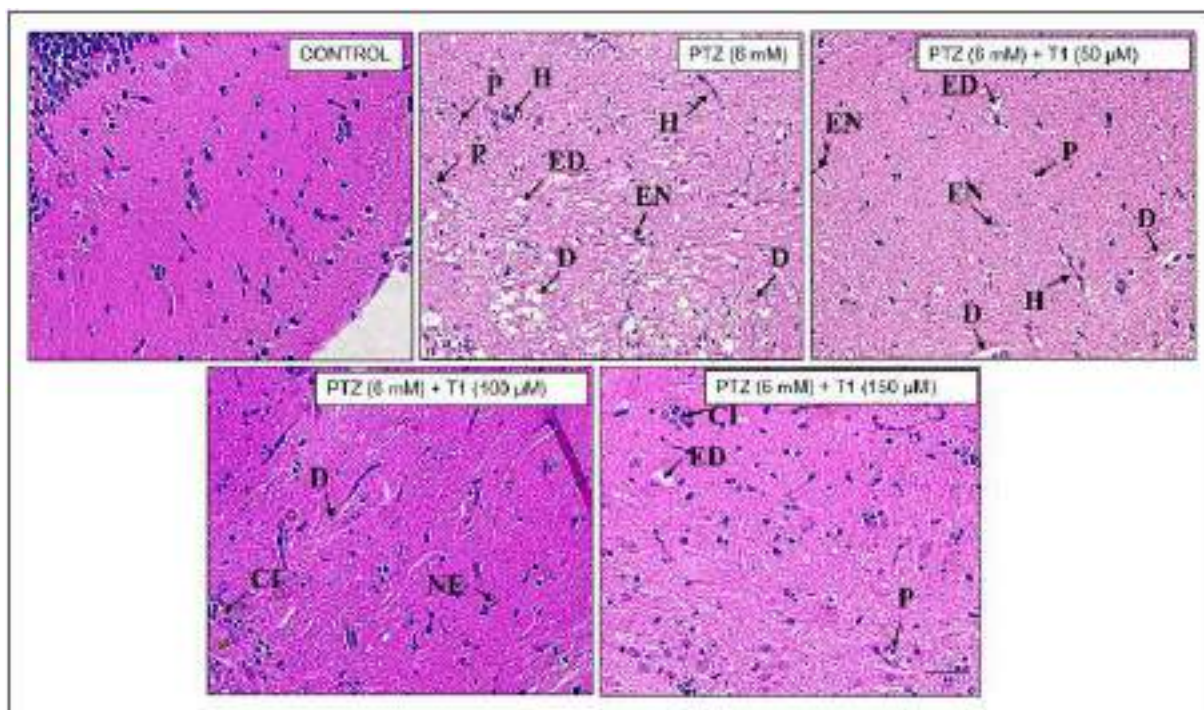


Fig. 6. Representative histological image of hematoxylin and eosin (H&E) staining of adult zebrafish brain from Control, PTZ (6 mM), and T1 at various concentrations (50, 100, and 150 μ M) groups. N: Nucleus, P: Pyknosis, H: Hemorrhage, ED: Edema, EN: Elongated Nucleus, D: Degeneration, CI: Cellular Infiltration. Scale- 50 μ m.

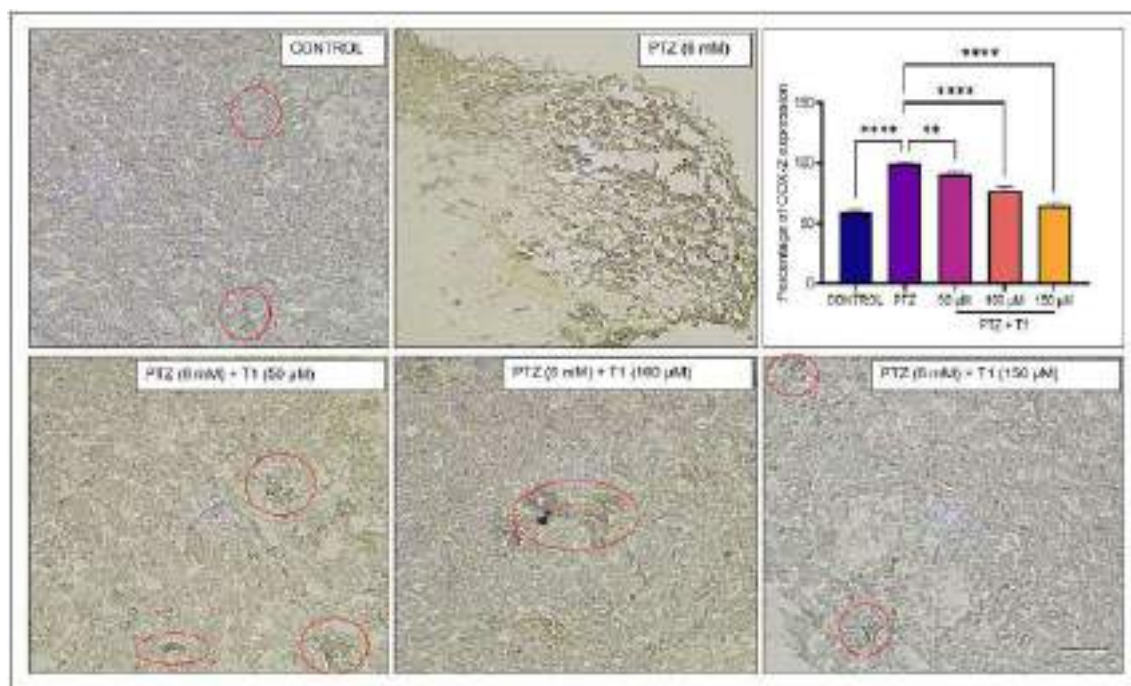


Fig. 7. Representative image for COX-2 expression from immunohistochemistry analysis in the brain of adult zebrafish from Control, PTZ (6 mM), and T1 at various concentrations (50, 100, and 150 μ M) groups. The graph depicts the percentage of fluorescent intensity calculated using ImageJ software. Data, derived from triplicate experiments, are presented as mean \pm standard deviation. Statistical analysis involved one-way ANOVA followed by Dunnett's multiple comparison test. *** signifies $p < 0.01$ and **** signifies $p < 0.0001$. Scale- 50 μ m.

3.8. T1 mitigates PTZ-induced behavioural changes

The results obtained from the behavioural analysis (Fig. 8) showed that the zebrafish in the PTZ group expressed alterations in behavioural

patterns such as swirling, creasing, and convulsions (please see Supplement Video S1). Whereas in T1 (150 μ M), the swirling, creasing as well as convulsant behaviour were significantly reduced. The total distance travelled by the zebrafish from PTZ was 2.63 ± 0.42 m. Whereas

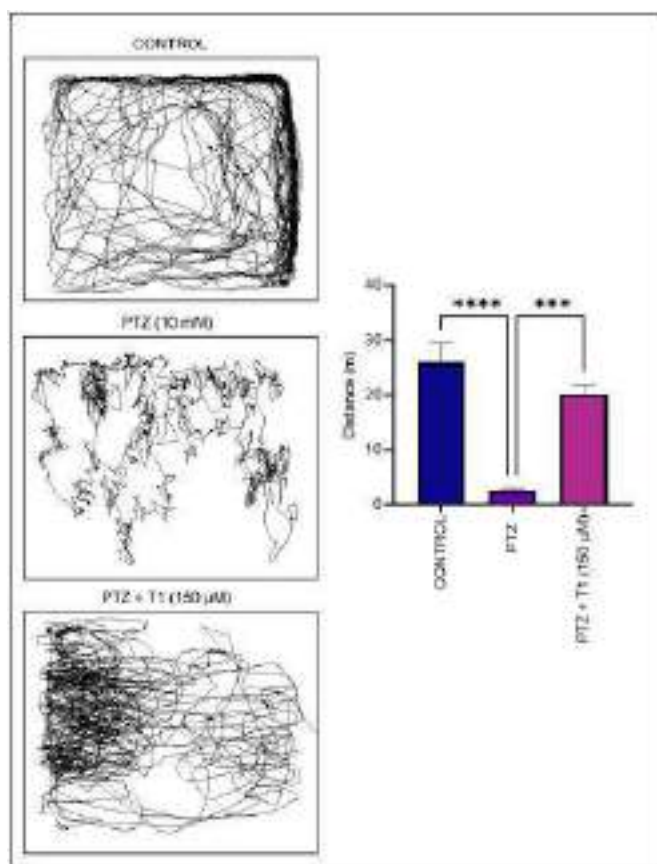


Fig. 8. Representative image of locomotion analysis through open-field test among zebrafish among experimental groups; Control, PTZ (6 mM), and T1 at 150 μ M concentration. The graph depicts the distance travelled by the zebrafish in meters. Data, derived from triplicate experiments, are presented as mean \pm standard deviation. Statistical analysis involved one-way ANOVA followed by Dunnett's multiple comparison test. '****' signifies $p < 0.001$ and '*****' signifies $p < 0.0001$.

in the T1 group, the total distance travelled by the zebrafish were significantly more to 20.11 ± 1.78 .

3.9. Activity of GABA increases by T1 treatment

The results obtained from HPLC-UV analysis (Fig. 9) showed that the level of GABA in the brain of PTZ-exposed zebrafish was significantly less compared with the control group. Whereas in T1 treated zebrafish, the level of GABA increased from 1.32 to 2.02 % at 150 μ M as compared to the control group.

4. Discussion

Epilepsy is a prevalent neurological disorder characterized by recurrent seizures and associated neurobiological and cognitive implications. The pathophysiological progression of epileptogenesis involves an inflammatory response within specific brain regions, precipitated by factors such as injury or the development of tumours [26]. In this current study, we used PTZ-induced kindling to develop the epilepsy-like condition in the zebrafish model. Furthermore, we investigated the protective effect of T1 derived from pyrazole benzenesulfonamide, which are best known for its anti-inflammatory potential [27]. PTZ instigates seizures by targeting GABA_A receptors associated with chloride ion channels. Previous studies have demonstrated elevated mortality in zebrafish larvae due to seizures induced by PTZ [28]. In line with these findings, our results indicate a notable increase in mortality rates in zebrafish larvae following PTZ exposure. Conversely, T1 pre-treatment exhibited a dose-dependent reduction in mortality rates, revealing the protective efficacy of T1 in this context.

To further elucidate the protective capacity of T1, we investigated the intracellular levels of ROS and apoptosis in zebrafish larvae. For instance, Taskiran et al previously documented an elevation in oxidative stress and apoptosis in neuronal cells (SH-SY5Y) and Wistar rats following exposure to PTZ [29]. Consistent with these findings, our current study reveals an augmentation in the levels of ROS and apoptosis in zebrafish larvae exposed to PTZ, as indicated by DCFDA analysis. Contrastingly, a dose-dependent reduction in intracellular ROS levels was observed in zebrafish larvae pre-treated with T1. Furthermore, the concentration-dependent decrease in apoptosis levels was evident in T1 pre-treated zebrafish larvae, signifying a potential mitigating effect of T1 on ROS-induced cellular stress and apoptosis in the context of PTZ exposure.

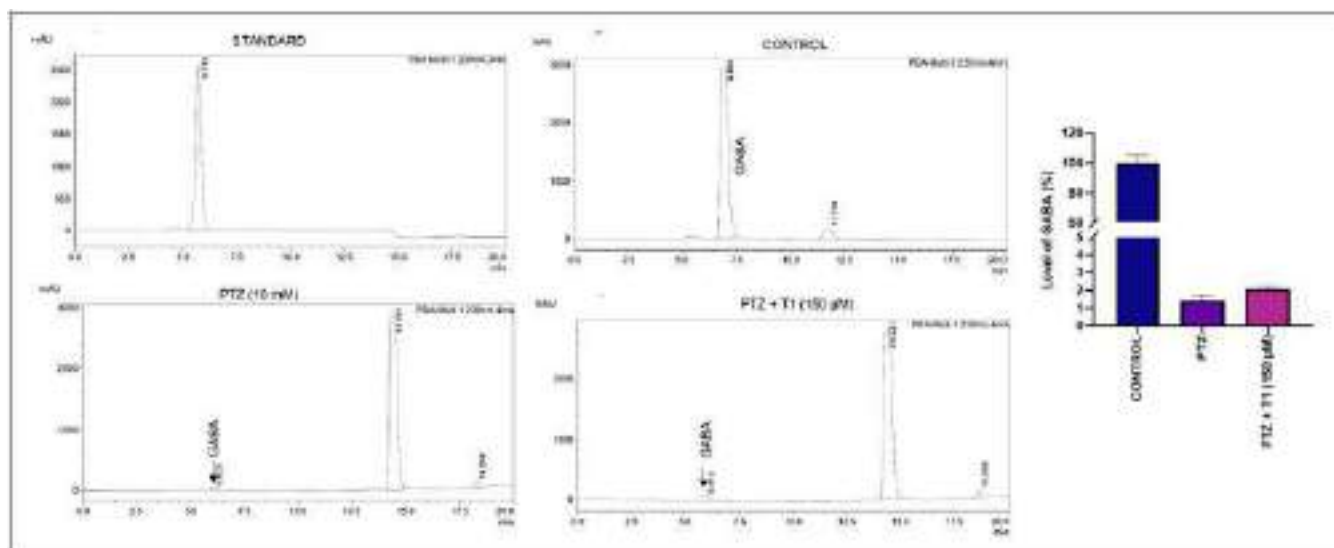


Fig. 9. Representative image for HPLC analysis for the detection of level of GABA in the brain of adult zebrafish among experimental groups; Control, PTZ (6 mM), and T1 at 150 μ M concentration.

Furthermore, the tissue damage in PTZ and T1 groups were analysed through histology technique in adult zebrafish. We found various abnormalities such as edema, neuronal degeneration and pyknosis in the brain tissue of PTZ exposed zebrafish. Whereas, T1 pre-treatment reduced the pyknosis and edema in brain tissue. Furthermore, the prevalent neuronal degeneration observed in PTZ-induced kindling models was attenuated in zebrafish subjected to pre-treatment with 150 μ M concentrations of T1. Concurrently, the RT-PCR analysis of *bndf* (brain-derived neurotrophic factor) gene expression aligns with these findings, revealing reduced expression of *bndf* in the PTZ group, contrasting with an increased expression observed in the T1 pre-treated groups. BDNF plays a vital role in growth and survival of neuronal cells [30]. Reduced expression of *bndf* in the PTZ group represents the dysfunction of the neuronal cell survival pathway, whereas in T1 pre-treatment groups, the decline of *bndf* gene expression was mitigated which supports the results from apoptosis and histology analysis. Altogether, these results suggest that treatment with T1 reduces the cellular damage caused by PTZ exposure in larvae and adult zebrafish.

PTZ, as a GABA_A receptor antagonist, causes a significant decline in the GABA levels of the zebrafish brain [31]. Hence, in the current study, we investigated the levels of GABA in PTZ-exposed larvae as well as in T1-treated larvae. The HPLC results however no significant difference by showing a slight increase in the concentration of GABA in the brain of zebrafish from the T1 treated group. Moreover, the results from the behavioural analysis showed a significant reduction in the Swirling, creasing and convulsant behaviour among the zebrafish from T1 (150 μ M) treated group. Together these results indicate that the convulsing behaviour of zebrafish was mitigated among zebrafish from the T1 group.

As mentioned earlier, the etiology of epilepsy accompanies inflammation due to damages inflicted in the seizure site. At normal physiological conditions, the inflammatory response generated during seizures is involved in repairing the damages inflicted. However, the epileptic condition deregulates the repair mechanism which sustains the inflammatory response [10]. The inflammatory response in zebrafish larvae was observed by locating the infiltrated macrophages. During inflammation in the brain, macrophage infiltration takes place which is then differentiated into microglia and astrocytes [32]. In the PTZ group, the number of localized macrophages was significantly higher compared to the control group, which indicates enhanced inflammation. Whereas, the T1 pre-treatment reduced the number of localised macrophages in concentration concentration-dependent manner. The localized macrophages such as microglia and astrocytes initialise the inflammatory response by secreting pro-inflammatory cytokines including IL-1 β , IL-6, and TNF- α [11]. This assertion is supported by the levels of *il-1 β* and *tnf- α* determined through RT-PCR analysis of zebrafish larvae in the PTZ group within the scope of the current study. Moreover, the outcomes derived from gene expression analysis demonstrated a dose-dependent reduction in the relative fold of pro-inflammatory genes expressed in zebrafish larvae pre-treated with varying concentrations of T1.

The generation of pro-inflammatory cytokines by microglia and astrocytes instigates the release of the COX-2 enzyme, subsequently activating the complement system [33]. Concurrently, RT-PCR analysis was employed to quantify the expression levels of the *cox-2* gene. The findings unveiled an upregulation of *cox-2* expression in zebrafish larvae subjected to PTZ exposure, indicative of an intensified complement system. In contrast, groups pre-treated with T1 exhibited a notable reduction in *cox-2* gene expression, particularly at higher concentrations (100 and 150 μ M). To corroborate these gene expression results, immunohistochemistry was utilized to evaluate COX-2 protein expression. The outcomes demonstrated a significant decline in COX-2 expression in the brains of adult zebrafish pre-treated with T1 at a concentration of 150 μ M. These findings underscore that T1 effectively mitigates the inflammatory response elicited by PTZ-induced seizures in both larval and adult zebrafish.

5. Conclusion

In summary, this current study provides valuable insights into the use of pyrazole benzenesulfonamide derivative molecule T1 against PTZ-induced epilepsy-like conditions. The robust evidence from gene expression and immunohistochemistry analyses supports the assertion that T1 effectively inhibits COX-2 and exhibits notable anti-inflammatory properties, reinforcing its potential as a targeted intervention. Additionally, the observed protective effects against cellular damages, as evidenced by mortality and cell damage analyses, underscore the compound's capacity to mitigate the detrimental impact of PTZ exposure on neuronal cells. The results from behavioural observation showed reduced convulsant behaviour among T1-treated zebrafish. While the modest influence on GABA levels suggests a nuanced impact on neuronal excitation signals, the overall findings collectively indicate T1's potential to mitigate neuronal damages, frequency of seizures and behavioural alterations imposed to zebrafish by epilepsy-like condition. Further investigations and clinical studies are warranted to unravel the full therapeutic potential of T1 in the context of epilepsy management and treatment.

6. Ethics approval and consent to participate

Animal experiments were performed as per the guidelines of the Committee for Control and Supervision of Experiments on Animals (CCSEA) and approved by the Institutional Animal Care and Use Committee of SRMIST (No. IAEC/312/2023).

7. Consent for publication

All of the authors give their consent for publication of the identifiable details of the text.

CRedit authorship contribution statement

Raghul Murugan: Writing – review & editing, Writing – original draft, Methodology, Investigation, Formal analysis, Data curation, Conceptualization. **S.P. Ramya Ranjan Nayak:** Methodology, Investigation, Formal analysis, Data curation. **B. Haridevamuthu:** Methodology, Investigation, Formal analysis, Data curation. **D. Priya:** Writing – original draft, Methodology, Investigation. **Vellapandian Chitra:** Investigation, Methodology, Resources, Writing – review & editing. **Bader O. Almutairi:** Writing – original draft, Resources, Methodology, Investigation. **Selvaraj Arokiyaraj:** Writing – original draft, Resources, Methodology, Investigation. **Muthupandian Saravanan:** Writing – original draft, Resources, Methodology, Investigation. **M.K. Kathiravan:** Writing – original draft, Resources, Methodology, Investigation. **Jesu Arockiaraj:** Writing – review & editing, Validation, Supervision, Resources, Project administration, Funding acquisition, Formal analysis, Data curation, Conceptualization.

Declaration of competing interest

The authors declare that they have no known competing financial interests or personal relationships that could have appeared to influence the work reported in this paper.

Data availability

Data will be made available on request.

Acknowledgment

The authors extend their sincere appreciation to Researchers Supporting Project Number (RSP2024R414), King Saud University, Riyadh, Saudi Arabia.

Appendix A. Supplementary data

Supplementary data to this article can be found online at <https://doi.org/10.1016/j.intimp.2024.111859>.

References

- [1] G.L. Sarlo, K.F. Holton, Brain concentrations of glutamate and GABA in human epilepsy: a review, *Seizure*. 91 (2021) 213–227, <https://doi.org/10.1016/j.seizure.2021.06.028>.
- [2] E. Beghi, The epidemiology of epilepsy, *Neuroepidemiology*. 54 (2020) 185–191, <https://doi.org/10.1159/000503831>.
- [3] A. Mobed, M. Shirafkan, S. Charsouei, J. Sadeghzadeh, A. Ahmadalipour, Biosensors technology for anti-epileptic drugs, *Clin. Chim. Acta*. 533 (2022) 175–182, <https://doi.org/10.1016/j.cca.2022.06.027>.
- [4] R. Falsaperla, G. D'Angelo, A.D. Praticò, L. Mauceri, M. Barbagallo, P. Pavone, S. Catanzaro, E. Gitto, G. Corsello, M. Ruggieri, Ketogenic diet for infants with epilepsy: a literature review, *Epilepsy Behav.* 112 (2020) 107361, <https://doi.org/10.1016/j.yebeh.2020.107361>.
- [5] Y. Wang, Z. Chen, An update for epilepsy research and antiepileptic drug development: Toward precise circuit therapy, *Pharmacol. Ther.* 201 (2019) 77–93, <https://doi.org/10.1016/j.pharmthera.2019.05.010>.
- [6] C.M. Cremer, N. Palomero-Gallagher, H.-J. Bidmon, A. Schleicher, E.-J. Speckmann, K. Zilles, Pentylentetrazole-induced seizures affect binding site densities for GABA, glutamate and adenosine receptors in the rat brain, *Neuroscience*. 163 (2009) 490–499, <https://doi.org/10.1016/j.neuroscience.2009.03.068>.
- [7] B.M. Radu, F.B. Epureanu, M. Radu, P.F. Fabene, G. Bertini, Nonsteroidal anti-inflammatory drugs in clinical and experimental epilepsy, *Epilepsy Res.* 131 (2017) 15–27, <https://doi.org/10.1016/j.epilepsyres.2017.02.003>.
- [8] J. Choi, D.R. Nordli, T.D. Alden, A. DiPatri, L. Laux, K. Kelley, J. Rosenow, S. U. Schuele, V. Rajaram, S. Koh, Cellular injury and neuroinflammation in children with chronic intractable epilepsy, *J. Neuroinflammation*. 6 (2009) 38, <https://doi.org/10.1186/1742-2094-6-38>.
- [9] A. Vezzani, A. Friedman, R.J. Dingledine, The role of inflammation in epileptogenesis, *Neuropharmacology*. 69 (2013) 16–24, <https://doi.org/10.1016/j.neuropharm.2012.04.004>.
- [10] A. Rana, A.E. Musto, The role of inflammation in the development of epilepsy, *J. Neuroinflammation*. 15 (2018) 144, <https://doi.org/10.1186/s12974-018-1192-7>.
- [11] A. Vezzani, J. French, T. Bartfai, T.Z. Baram, The role of inflammation in epilepsy, *Nat. Rev. Neurol.* 7 (2011) 31–40, <https://doi.org/10.1038/nrneurol.2010.178>.
- [12] G. El-Saber Batiha, A. Magdy Beshbishy, A. El-Mleeh, M.M. Abdel-Daim, H. Prasad Devkota, Traditional uses, bioactive chemical constituents, and Pharmacological and toxicological activities of *Glycyrrhiza glabra* L. (fabaceae), *Biomolecules*. 10 (2020) 352, <https://doi.org/10.3390/biom10030352>.
- [13] M.-A.-A. El-Sayed, N.I. Abdel-Aziz, A.-A.-M. Abdel-Aziz, A.S. El-Azab, K.E. H. ElTahir, Synthesis, biological evaluation and molecular modeling study of pyrazole and pyrazoline derivatives as selective COX-2 inhibitors and anti-inflammatory agents. Part 2, *Bioorg. Med. Chem.* 20 (2012) 3306–3316, <https://doi.org/10.1016/j.bmc.2012.03.044>.
- [14] A. Balbi, M.E. Anzaldi, C. Macciò, C. Aiello, M. Mazzei, R. Gangemi, P. Castagnola, M. Miele, C. Rosano, M. Viale, Synthesis and biological evaluation of novel pyrazole derivatives with anticancer activity, *Eur. J. Med. Chem.* 46 (2011) 5293–5309, <https://doi.org/10.1016/j.ejmech.2011.08.014>.
- [15] D. Priya, M.K. Kathiravan, Molecular insights into benzene sulphonamide substituted diarylpyrazoles as cyclooxygenase-2 inhibitor and its structural modifications, *J. Biomol. Struct. Dyn.* 39 (2021) 5093–5104, <https://doi.org/10.1080/07391102.2020.1785329>.
- [16] B. Haridevamuthu, R. Murugan, B. Seenivasan, R. Meenatchi, R. Pachaiappan, B. O. Almutairi, S. Arokiyaraj, J. Arockiaraj, Synthetic azo-dye, Tartrazine induces neurodevelopmental toxicity via mitochondria-mediated apoptosis in zebrafish embryos, *J. Hazard. Mater.* 461 (2024) 132524, <https://doi.org/10.1016/j.jhazmat.2023.132524>.
- [17] B. Haridevamuthu, T. Manjunathan, A. Guru, C. Ranjith Wilson Alphonse, S. Boopathi, R. Murugan, M.K. Gatasheh, A. Atef Hatamleh, A. Juliet, P. Gopinath, J. Arockiaraj, Amelioration of acrylamide induced neurotoxicity by benzo[b]thiophene analogs via glutathione redox dynamics in zebrafish larvae, *Brain Res.* 1788 (2022) 147941, doi: 10.1016/j.brainres.2022.147941.
- [18] R. Murugan, R. Rajesh, A. Guru, B. Haridevamuthu, B.O. Almutairi, M. H. Almutairi, A. Juliet, S. Renganayagi, P. Gopinath, J. Arockiaraj, Deacetyloxyazadiradione derived from epoxyazadiradione of neem (*Azadirachta indica* a. juss) fruits mitigates LPS-induced oxidative stress and inflammation in zebrafish larvae, *Chem. Biodivers.* 19 (2022), <https://doi.org/10.1002/cbdv.202200041>.
- [19] R. Murugan, R. Rajesh, B. Seenivasan, B. Haridevamuthu, G. Sudhakaran, A. Guru, R. Rajagopal, P. Kuppusamy, A. Juliet, P. Priya, S. Muthuraman, R.S. Kumar, K. Manikandan, B.O. Almutairi, M.H. Almutairi, S. Arokiyaraj, P. Gopinath, J. Arockiaraj, Hepatoprotective effect of dihydroxy piperlongumine in high cholesterol-induced non-alcoholic fatty liver disease zebrafish via antioxidant activity, *Eur. J. Pharmacol.* 945 (2023) 175605, <https://doi.org/10.1016/j.ejphar.2023.175605>.
- [20] E.-A. Kim, S.-Y. Kim, B.-R. Ye, J. Kim, S.-C. Ko, W.W. Lee, K.-N. Kim, I.-W. Choi, W.-K. Jung, S.-J. Heo, Anti-inflammatory effect of Apo-9'-fucosanthinone via inhibition of MAPKs and NF- κ B signaling pathway in LPS-stimulated RAW 264.7 macrophages and zebrafish model, *Int. Immunopharmacol.* 59 (2018) 339–346, <https://doi.org/10.1016/j.intimp.2018.03.034>.
- [21] B. Haridevamuthu, B. Seenivasan, P.S. Priya, S. Muthuraman, R.S. Kumar, K. Manikandan, B.O. Almutairi, M.H. Almutairi, S. Arokiyaraj, P. Gopinath, J. Arockiaraj, Hepatoprotective effect of dihydroxy piperlongumine in high cholesterol-induced non-alcoholic fatty liver disease zebrafish via antioxidant activity, *Eur. J. Pharmacol.* 945 (2023) 175605, <https://doi.org/10.1016/j.ejphar.2023.175605>.
- [22] A. Khaleel, A.R. El-Sheakh, G.M. Suddek, Celecoxib abrogates concanavalin A-induced hepatitis in mice: possible involvement of Nrf2/HO-1, JNK signaling pathways and COX-2 expression, *Int. Immunopharmacol.* 121 (2023) 110442, <https://doi.org/10.1016/j.intimp.2023.110442>.
- [23] S.P.R.R. Nayak, S. Boopathi, P.S. Priya, M. Pasupuleti, R. Pachaiappan, B. O. Almutairi, S. Arokiyaraj, J. Arockiaraj, Luteolin, a promising quorum quencher mitigates virulence factors production in *Pseudomonas aeruginosa* - in vitro and in vivo approach, *Microb. Pathog.* 180 (2023) 106123, <https://doi.org/10.1016/j.micpath.2023.106123>.
- [24] S.E. Wirbisky, G.J. Weber, M.S. Sepúlveda, C. Xiao, J.R. Cannon, J.L. Freeman, Developmental origins of neurotransmitter and transcriptome alterations in adult female zebrafish exposed to atrazine during embryogenesis, *Toxicology*. 333 (2015) 156–167, <https://doi.org/10.1016/j.tox.2015.04.016>.
- [25] Y. Lü, H. Zhang, X. Meng, L. Wang, X. Guo, A validated HPLC method for the determination of GABA by pre-column derivatization with 2,4-dinitrofluorodinitrobenzene and its application to plant GAD activity study, *Anal. Lett.* 43 (2010) 2663–2671, <https://doi.org/10.1080/00032711003763558>.
- [26] R.D. Thijs, R. Surges, T.J. O'Brien, J.W. Sander, Epilepsy in adults, *Lancet*. 393 (2015) 689–701, [https://doi.org/10.1016/S0140-6736\(15\)32596-0](https://doi.org/10.1016/S0140-6736(15)32596-0).
- [27] D. Priya, P. Gopinath, L.S. Dhivya, A. Vijayababu, M. Haritha, S. Palaniappan, M. K. Kathiravan, Structural insights into pyrazoles as agents against anti-inflammatory and related Disorders, *ChemistrySelect*. 7 (2022), <https://doi.org/10.1002/slct.202104429>.
- [28] M.N.V. Gwedela, H. Terai, F. Lampiao, K. Matsunami, H. Aizawa, Anti-seizure effects of medicinal plants in Malawi on pentylentetrazole-induced seizures in zebrafish larvae, *J. Ethnopharmacol.* 284 (2022) 114763, <https://doi.org/10.1016/j.jep.2021.114763>.
- [29] A.S. Taskiran, M. Ergul, The modulator action of thiamine against pentylentetrazole-induced seizures, apoptosis, nitric oxide, and oxidative stress in rats and SH-SY5Y neuronal cell line, *Chem. Biol. Interact.* 340 (2021) 109447, <https://doi.org/10.1016/j.cbi.2021.109447>.
- [30] S. Bathina, U.N. Das, Brain-derived neurotrophic factor and its clinical implications, *Arch. Med. Sci.* 6 (2015) 1164–1178, <https://doi.org/10.5114/aoms.2015.56342>.
- [31] K. Gawel, W. Kukula-Koch, N.S. Banono, D. Nieoczym, K.M. Targowska-Duda, L. Czernicka, J. Parada-Turska, C.V. Esquerro, 6-gingerol, a major constituent of *Zingiber officinale* rhizoma, exerts anticonvulsant activity in the pentylentetrazole-induced seizure model in Larval zebrafish, *Int. J. Mol. Sci.* 22 (2021) 7745, <https://doi.org/10.3390/ijms22147745>.
- [32] A.D. Greenhalgh, J.G. Zaruk, L.M. Healy, S.J. Baskar Jesudasan, P. Jhelum, C. K. Salmon, A. Formanek, M.V. Russo, J.P. Antel, D.B. McGavern, B.W. McColl, S. David, Peripherally derived macrophages modulate microglial function to reduce inflammation after CNS injury, *PLOS Biol.* 16 (2018) e2005264.
- [33] L. Minghetti, Cyclooxygenase-2 (COX-2) in inflammatory and degenerative brain diseases, *J. Neuropathol. Exp. Neurol.* 63 (2004) 901–910, <https://doi.org/10.1093/jnen/63.9.901>.